A Validation and Uncertainty Quantification Framework for Eulerian-Eulerian Two-Fluid Model based Multiphase-CFD Solver. Part I: Methodology

Yang Liu[1,*], Nam Dinh[1], Ralph Smith[2]

1 Department of Nuclear Engineering, North Carolina State University, Raleigh, NC 27606, USA

2 Department of Mathematics, North Carolina State University, Raleigh, NC 27607, USA

Abstract

In this paper, a validation and uncertainty quantification (VUQ) framework for the Eulerian-Eulerian two-fluid-model based multiphase-computational fluid dynamics solver (MCFD) is formulated. The framework aims to answer the question: how to evaluate if a MCFD solver adequately represents the underlying physics of a multiphase system of interest? The proposed framework is based on total data-model integration (TDMI) approach that uses Bayesian method to inversely quantify the uncertainty of the solver predictions with the support of multiple experimental datasets. The framework consists of six steps with state-of-the-art statistical methods, including: 1). Solver evaluation and data collection; 2). Surrogate model construction; 3). Sensitivity Analysis; 4). Parameter selection; 5). Uncertainty quantification with Bayesian inference; and 6). Validation metrics calculation. Those steps are formulated in a modular manner and using non-intrusive methods. Such features ensure the applicability of the flexible framework to different scenarios and modeling of multiphase flow and boiling heat transfer, as well as the extensibility of the framework to support VUQ of different MCFD solvers.

1. Introduction

Two-phase flow and boiling are used for thermal management in various engineered systems with high energy density, from power electronics to heat exchangers in power plants and nuclear reactors. It is important to understand the complex phenomena involves in those systems. The experimental study of two-phase flow and boiling at large, industrial scales are technically challenging and expensive. Thus the design and safety analysis of those systems are highly dependent on the scientific simulation tools.

For applications with complex geometries such as reactor fuel rod bundle, the Multiphase Computational Fluid Dynamics (MCFD) based on Eulerian-Eulerian two-fluid-model is a promising tool. One of the major advantages of two-fluid-model based solver is that it averaged the interface information between vapor and liquid, thus significantly reduces the computation requirement compared to the first-principal simulation method such as Volume of Fluid (VOF) or Interface Tracking Method (ITM). Based on this reason MCFD method attracts increasingly

* Corresponding author.

Email address: yliu73@ncsu.edu (Y.Liu), ntdinh@ncsu.edu (N.Dinh), rsmith@ncsu.edu(R.Smith)

interests over recent two decades, from general bubbly flow and boiling simulation such as the work of (Sugrue et al., 2017) and (Krepper et al., 2007) to critical heat flux prediction (Yadigaroglu, 2014), (Mimouni et al., 2016). On the other hand, however, the interfacial average process also cause a loss of information, and closure relations needs to be introduced in the conservative equations to make them solvable. For example, a MCFD solver requires wall boiling closure relations to describe the boiling process happen on the wall. It also requires the interfacial mass, energy, and momentum exchange closure relations to compensate the information loss in the interface average process. There are two issues for applying those closure relations in a MCFD solver. Firstly, most of those closure relations are empirical or semi-empirical correlations with empirical parameters whose values significantly influence the results of the solver, yet the values of those parameters can vary significantly between different practices. Secondly, the closure relations are proposed in a manner that one closure relation deals with only one physical phenomena, a group of closure relations are then assembled for the whole system. Such "divide-and-conquer" approach neglects the possible interactions between different closure relations. Such limitations put additional challenge to the predicative capability of the MCFD solver. Compared to the single case study, a more desired approach to validate the solver is to assess its predictions over a broad range of conditions with the support of experimental measurements, as discussed in (Colombo and Fairweather,2016). Such assessment can be further extended to a more rigorous validation and uncertainty quantification (VUQ) process which measures the agreement between model predictions and experimental data by quantifying the uncertainties of the model predictions.

VUQ is an active research topic in both statistics community and scientific simulation community. There are several statistical methods that can be applied to the Uncertainty Quantification (UQ) as summarized in the book by (Smith, 2014). The different aspects of the validation process for scientific simulations are studied and discussed in (Oberkampf and Roy,2010). There are several definitions of validation that have been used in different communities, one of the most well-known definition is included in (Oberkampf and Roy,2010) which defines validation as:

- *The process of determining the degree to which a model is an accurate representation of the real world from the perspective of the intended uses of the model.*

To evaluate such accuracy of a model, a natural first step is to understand the uncertainties of its predictions, as well as the source of those uncertainties. In this sense, the uncertainty quantification of a model is always tightly connected with the validation of it; thus the validation and uncertainty quantification are always discussed in an integrated manner.

Currently, applications of validation or uncertainty quantification can be found in many branches of scientific simulation (Wu and Kozlowski,2017), (Avramova and Ivanov,2010), (Donato and Pitchumani,2014). Several VUQ related works have also been applied to MCFD solver. (Picchi and Poesio,2017) applied Sobol indices for GSA and Monte Carlo sampling method for forward UQ on flow pattern transition boundaries in one-dimensional two-fluid-model. (Ren et al., 2017) applied the Bayesian method to select different set of closure relations in multiphase flow in porous media. (Yurko et al., 2015) applied emulator based Bayesian calibration on nuclear reactor system analysis code. (Wu et al., 2017) use Bayesian method to perform inverse UQ on the 1-dimensional nuclear reactor system code TRACE with

different surrogate model construction methods. Using statistical learning method, (Ma et al., 2016) constructed a neural network based closure relation to represent the interfacial force in MCFD solver that learned from DNS data.

On the other hand, the comprehensive VUQ practices on MCFD solver are still very limited due to several difficulties:

- For a given scenario, there are multiple Quantities of Interest (QoIs) predicted by the solver, e.g. temperature, velocity, void fraction, heat transfer. Many of those QoIs are tightly coupled and demand to be treated in an integrated manner. For example, one cannot perform validation on void fraction while neglecting the phasic velocities. Moreover, those QoIs is given by the solver in the form of spatial distributions (for transient problems, they are also in the form of temporal distributions), which results in high dimensional outputs of those QoIs.
- The two-fluid-model based MCFD solver is still relatively computationally expensive. For VUQ practices based on statistical methods such as Bayesian inference or Monte Carlo sampling, it usually takes tens of thousands of solver evaluations with varied parameter values. It is computationally prohibitive to directly run the MCFD these many times.
- The detailed measurement of multiphase flow is difficult, thus there are not have enough available experimental data to support the VUQ practice. Expert opinion based on experience and prior knowledge is necessary to compensate the scarcity of data.

To overcome those difficulties, a VUQ framework is proposed in this work. This framework is designed for the computational model that has the following features: relies on empirical parameters, gives multiple QoIs predictions in spatial or temporal distributions, and has limited experimental measurement supports. The work is demonstrated in a two-part paper, the first part discusses the proposed VUQ framework and the relevant methods and algorithms, and the second part demonstrates the cases studies of the framework. This first part is organized in the following structure. Section 2 discusses the current efforts on the VUQ work, in the perspective of CFD community as well as statistics community. Section 3 reviews the two-fluid-model based MCFD solver with a comprehensive closure structure evaluation. Section 4 introduces the VUQ framework we proposed step-by-step. Section 5 discusses the summary remarks of the framework.

2. Literature review on VUQ works

2.1 General ideas and characterization of VUQ

The first step and the major component of a comprehensive VUQ work is to quantify the uncertainties of the model predictions. For a general computational model, there are three uncertainty sources:

- Model parameter uncertainty. A computational model inevitably contains parameters that need to be specified before the model can be used for prediction. Those parameters, whether denoting certain input physical quantities such as inlet velocity or wall heat flux, or representing the empirical description of a closure relation, have uncertainties that influence the prediction. Such uncertainty can come from the intrinsic variation of

the physical process such as the fluctuation of inlet velocity, or the lack of knowledge about a certain phenomenon such as the empirical parameter in a closure relation. In this sense, those parameters are treated as random variables if the UQ is performed under the Bayesian framework. Uncertainty introduced by those parameters are termed as model parameter uncertainties, which needs to be quantified and then propagated through the model.

- Model form uncertainties. The model form uncertainty is also termed as *model bias*, *model inadequacy*, or *model discrepancy* in different references. It stems from the simple fact that no model is perfect. This occurs even for a model with no parameter uncertainty so that the true values of all parameters required for a model are known. With all those true parameter values, the obtained QoIs from the model still would not be their true values in the real world. Such discrepancy is embedded in the formulation of the model, which usually includes approximations and simplifications for certain complicated physics, as well as ignorance of some physical interactions between different phenomena, especially for complicated multi-scale problems such as the multiphase flow and boiling. The model form uncertainty is generally problem dependent and more difficult to address as compared to the parameter uncertainty. The study of the model form uncertainty is a topic of active research.
- Numerical errors and uncertainties. The numerical errors mainly arise from the discretization process and maps the continuum PDE to discrete equations, insufficient iterative convergence for solving the nonlinear equations, as well as the round-off of simulation results. Strictly speaking, the evaluation of numerical errors is not considered a work of validation, but a work of solution verification, which evaluates the numerical accuracy of the computational model.

The UQ process can be further characterized as two different types: the forward UQ and the inverse UQ. The first type is based on the assumption that the model parameter uncertainties are already known. Thus the probability distributions of the QoIs can be obtained by simply perturbing the parameter values according to their known distributions. This can be done with the Monte Carlo method with certain sampling strategies such as Latin Hypercube Sampling (LHS). In most practices of forward UQ, the experimental data is not directly evolved. This process is usually applied to problems that only evolve measurable parameters with clear knowledge. The inverse UQ, on the other hand, is based on a more realistic assumption that we have limited knowledge of the parameters implemented in the model. Thus, the uncertainties of the parameters need to be inferred using experimental measurements. The Bayesian framework is a suitable statistical tool for such inference and has multiple applications since it was firstly introduced for computational models by (Kennedy and O'Hagan,2001). The Bayesian framework assumes that parameters can be regarded as random variables, and have prior distributions based on current knowledge about it. With the experimental data, the likelihood function can be calculated. Combing this likelihood function with the prior distribution, the posterior distribution can be obtained. The likelihood term takes into account how probable the data is given the parameters of the model. Once the posterior distribution of the parameter is obtained, it can be propagated through the model to construct uncertainties of QoIs using forward UQ. In the inverse UQ, the model form uncertainty can be considered. For

problems with empirical parameters that cannot be directly measured, inverse UQ needs to be applied.

Once the uncertainty of QoIs are quantified, the next questions would be how to evaluate the agreement between those simulation results and the experimental measurements? The most straightforward, and most commonly used in engineering community, approach is to directly display the simulation results and data on a graph. Such comparison, while providing a basic understanding of the model accuracy, cannot generate a comprehensive measure of the model-data discrepancy. Moreover, the model uncertainty and the experiment uncertainty are neglected in this type of treatment. As an improvement, several validation metrics are proposed to give a more rigorous evaluation of the model-data agreement. There are certain desired features of a good validation metrics as suggested by (Y. Liu et al., 2011). First and foremost, a good validation metric should be quantitative rather than qualitative. Secondly, a validation metric should be objective. Once the predicted QoIs and the experimental data are given (with their uncertainties), the metric will produce the same result no matter of who conducted the assessment. A validation metric should also take into account the full uncertainty distribution of both the predictions and the experimental data, rather than simply compare their mean values.

Generally speaking, validation metrics currently applied to scientific computation problems can be characterized into three categories. The first type is hypothesis testing. In this type of validation metric, two hypotheses are constructed. The first one is called null hypothesis which is initially assumed to be true and usually it is set to be "the model is in agreement with the observed data". The second one is called alternative hypothesis, which contradicts the null hypothesis, such as "the model is not in agreement with the observed data". Hypothesis testing based on the observed data to construct a test statistics *S* based on which to decide whether to accept or reject the null hypothesis, thus the outcome of this type of validation metric is only a "Yes or No" statement. The second type is Confidence Interval (CI) proposed by (Oberkampf and Barone,2006) which measures the discrepancy between the mean of predicted QoIs and the experimental data, plus the uncertainty of measurement. The confidence interval can be constructed as

$$\left(\tilde{\mathbf{E}} - t_{\alpha/2,v} \cdot \frac{\mathbf{s}}{\sqrt{n}}, \tilde{\mathbf{E}} + t_{\alpha/2,v} \cdot \frac{\mathbf{s}}{\sqrt{n}}\right), \tag{1}$$

where $\tilde{\mathbf{E}}$ is the estimated error between model and data,

$$\tilde{\mathbf{E}} = \mathbf{y}^M(\mathbf{x}, \mathbf{v}, \overline{\boldsymbol{\theta}}_{post}) - \bar{\mathbf{y}}^E(\mathbf{x}, \mathbf{v}) \tag{2}$$

s is the standard deviation of the experimental data, $t_{\alpha/2,v}$ is the 1-α/2 quantile of the t-distribution with freedom of *v* used to quantify the uncertainty of experimental data. The obtained CI can be interpreted as "we have $(1-\alpha)\times 100\%$ confidence that the true discrepancy between model and observed data is within the interval".

The third type is termed area metric, which is proposed by (Ferson et al., 2008). In this type of validation metric, both the experimental data and model predicted QoIs are treated as random variables, whose probability distribution is their uncertainty distribution. The area metric measures the area between the two Cumulative Distribution Functions (CDFs), which can be expressed as

$$d\left(F_{x_i}^E, F_{x_i}^M\right) = \int_{-\infty}^{+\infty} \left|F_{x_i}^E(x) - F_{x_i}^M(x)\right| dx \,. \quad (3)$$

One of a major merit of the area metric is that it takes the full uncertainty distribution of both data and model prediction into consideration. It also needs to mention that there are also other forms of validation metrics such as u-pooling and p-box (Ferson and Oberkampf,2009) which are extensions of the area metrics.

2.2 Statistical methods related to VUQ

As previously mentioned, the Bayesian framework is widely used for the inverse UQ problem. It combines the prior knowledge (in the form of prior distribution) and current evidence (in the form of likelihood function) about the empirical parameters and produces the posterior distributions for them. The Bayesian framework is naturally compatible to deal with multiple QoIs which makes it a promising tool for the VUQ work of MCFD solver.

Applying Bayesian methods to quantify multiple uncertainty sources of computational models is first introduced by (Kennedy and O'Hagan,2001). In the work, the idea of performing Bayesian inference on Gaussian Process based surrogate model was proposed with an application of radioactive materials deposition in an accident. Based on this work, (Bayarri et al., 2007) proposed a validation framework for a simple computational model (with an example regarding spot welding model). (Higdon et al., 2004) and (F. Liu et al., 2008) applied the work to thermal problems. This work was more focused on developing statistical methods, the model studied was heat conduction, a simple physical process. (Higdon et al., 2008) further extended the work to models with high dimensional outputs using dimension reduction methods. In those works, the model form uncertainty was considered as a bias term δ which is considered using the data-driven approach with details discussed in Section 4.5.

For complicated problems, such as multiphase flow and boiling, the number of closure relations and empirical parameters implemented in the solver is usually large. Directly applying Bayesian methods on all of them is not only inefficient but also introducing the "parameter identifiability" issue. For such problems, the Global Sensitivity Analysis (GSA) can be used to identify the parameters that have significant influences on the model predictions over the whole admissible space. Then only the influential parameters will be selected for the Bayesian inference. Two methods can be applied for the GSA, the Morris screening method developed by (Morris, 1991) and variance based method developed by (Sobol, 2001), the details will be discussed in Section 4.3. For some problems, even the influential parameters cannot be identified against each other, then more rigorous algorithms should be applied, the details is discussed in section 4.4.

2.3 Validation practices in CFD community

The validation of CFD has been studied for at least two decades (Roache, 1997), (Oberkampf and Trucano,2002). A validation framework has been formulated (AIAA, 1998), including construction of validation hierarchy, design of validation experiments, UQ in computations, and validation metrics. The fundamental idea of the validation framework is phenomena

decomposition, which is similar to the “divide-and-conquer” approach for the closure development in MCFD solver. It decomposes a complex system studied by CFD into several progressively simpler tiers. Each tier represents a series of sub-systems or phenomena of the complete system; an example is given in Figure 1. Validation experiments need to be conducted according to the decomposition which should provide measurements for all the inputs and outputs of the components. This framework provides detailed guidance with solid theoretical background for the CFD validation. However, based on the authors’ best knowledge, there is no engineering application that follows the complete process of the validation framework. The major difficulty is the limitation of data. To support the validation work, a new type of experiment termed validation experiment is required whose most updated criteria are evaluated in (Oberkampf and Smith,2017). Comparing to validation experiments, the data obtained from current traditional experiments only contains incomplete information and thus is considered to be insufficient to serve the validation purpose. In this sense, design a more flexible validation framework that is compatible with the traditional experiment is the focus of this paper. The proposed approach is to couple validation with the UQ process

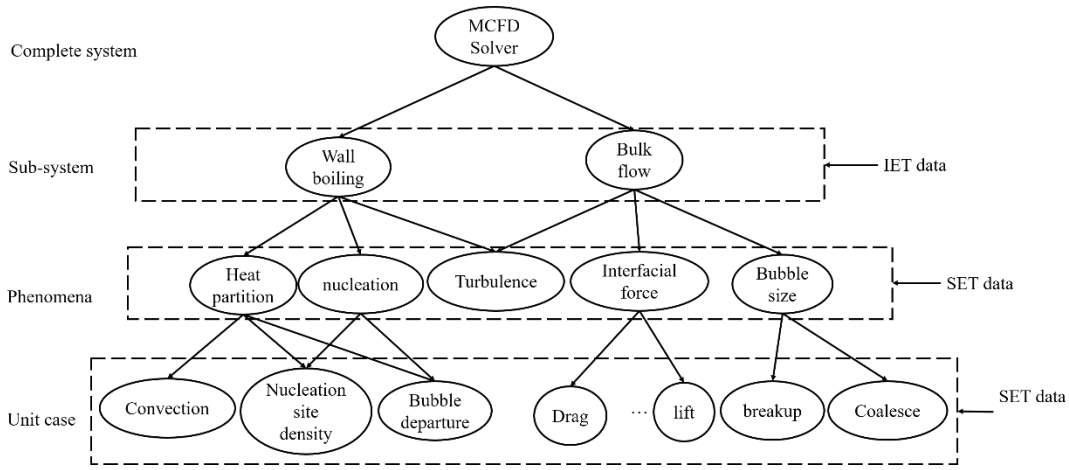

Figure 1. Validation hierarchy for MCFD solver based on AIAA guidance

For the validation of MCFD solver, another difficulty regarding to VUQ are the closure relations and empirical parameters in the solver. Works of (Rzehak and Krepper,2013) studied the parametric effects of multiple closure relations in subcooled flow boiling problems using commercial CFD code CFX and performed validation of simulation results against experimental data. (Q. Wang and Yao,2016) studied the interfacial forces closure relations in MCFD solver and validated the results against bubbly flow experimental data. Significant influence of parameter variations on the model predictions has been observed in those practices. Such works demonstrate the necessity to take special attention on the empirical parameter in the VUQ study.

3. MCFD solver based on Eulerian-Eulerian two-fluid-model

The fundamental idea of a two-fluid-model is to average the local instantaneous conservation equations, thus eliminating the need for tracking interfaces to achieve computational efficiency. The system of averaged conservation equations needs to be solved numerically, commonly using a finite-volume or finite-element method. The convergence and accuracy of the solution depend on numerical techniques and temporal and spatial resolutions needed to capture the dynamics and scales of governing physical processes.

3.1 Conservative equations

Generally speaking, the two-fluid model solver relies on solving three ensemble averaged conservative equations for mass, momentum and energy. The k-phasic mass conservation equation can be written as

$$\frac{\partial(\alpha_k \rho_k)}{\partial t} + \nabla \cdot (\alpha_k \rho_k \mathbf{U}_k) = \Gamma_{ki} - \Gamma_{ik} \tag{4}$$

where the two terms on the left-hand side represent the rate of change and convection, the two terms on the right-hand side represent the rate of mass exchanges between phases due to condensation and evaporation.

The k-phasic momentum equation is given by

$$\frac{\partial(\alpha_k \rho_k \mathbf{U}_k)}{\partial t} + \nabla \cdot (\alpha_k \rho_k \mathbf{U}_k \mathbf{U}_k) = -\alpha_k \nabla p_k + \nabla \cdot [\alpha_k (\tau_k + \tau_k^t)] + \alpha_k \rho_k \mathbf{g} + \Gamma_{ki} \mathbf{U}_i - \Gamma_{ki} \mathbf{U}_k + \mathbf{M}_{ki}, \tag{5}$$

where *i* represents the interphase between two phases, $\mathbf{M}_{ki}$ represents the term of averaged interfacial momentum exchange, which can be modeled by a set of interfacial force closure relations.

The k-phasic energy conservation equation in terms of specific enthalpy can be given as

$$\frac{\partial(\alpha_k \rho_k h_k)}{\partial t} + \nabla \cdot (\alpha_k \rho_k h_k \mathbf{U}_k) = \nabla \cdot \left[\alpha_k \left(\lambda_k \nabla T_k - \frac{\mu_k}{\mathrm{Pr}_k^t} \nabla h_k\right)\right] + \alpha_k \frac{Dp}{Dt} + \Gamma_{ki} h_i - \Gamma_{ik} h_k + q_k \,, \tag{6}$$

where the terms on the right-hand side represent heat transfer in phase *k,* work done by pressure, enthalpy change due to evaporation and condensation, and heat flux from the wall. The wall boiling heat transfer is modeled by a set of closure relations.

3.2 Characterization of Closure relations in MCFD

Solving a typical two-phase flow and boiling problem involves predicting the boiling process on the heated wall and flow and heat transfer process in the bulk flow. The boiling process involves complex multi-physics process that includes interaction between liquid and the wall surface, such as nucleation and bubble departure. Such process cannot be directly resolved in the MCFD solver. Thus, wall boiling closure relations are incorporated in the MCFD solver to predict the boiling process; some recent development also includes the capability for the prediction of the departure from nucleate boiling (DNB) (Mimouni et al., 2016), (Gilman and Baglietto,2017). After nucleation and departure from the wall, the bubbles join the bulk flow

and interacting with the liquid in the bulk flow. Resolving such interactions require a series of closure relations for the interphase exchange of mass, momentum and energy. Interfacial force closure relations are proposed to describe the interphase momentum exchange, while interfacial condensation closure is necessary to describe the interphase mass and heat transfer for the subcooled flow boiling problem. Moreover, the size of bubbles has significant influence on those interphase exchanges, and closure relation is needed for determining the bubble size. Last, the turbulence can influence the interphase exchange, and the bubble dynamics in turn influences the turbulence, thus closure relation is also required to describe the bubble-induced turbulence. Thus the closure relations in a MCFD solver can be characterized into five categories: wall boiling, interfacial momentum exchange, interfacial mass/heat transfer, bubble size, and turbulence. There exist complex relationships between those closure relations and a typical structure of them is depicted in Figure 2. The role of closure relation is the reflection of the "divide-and-conquer" philosophy that decompose a complex system into several sub-phenomena and models them with closure relations separately. It should also be noted that most of those closure relations are proposed for bubbly flow which assumes the continuous phase is liquid and the disperse phase is vapor or gas. Several investigations also assume such closure relations can be extended to droplet flow simulation where the continuous phase is vapor while disperse phase is liquid droplet. There are still gaps for the modeling of slug or churn flow using MCFD solver.

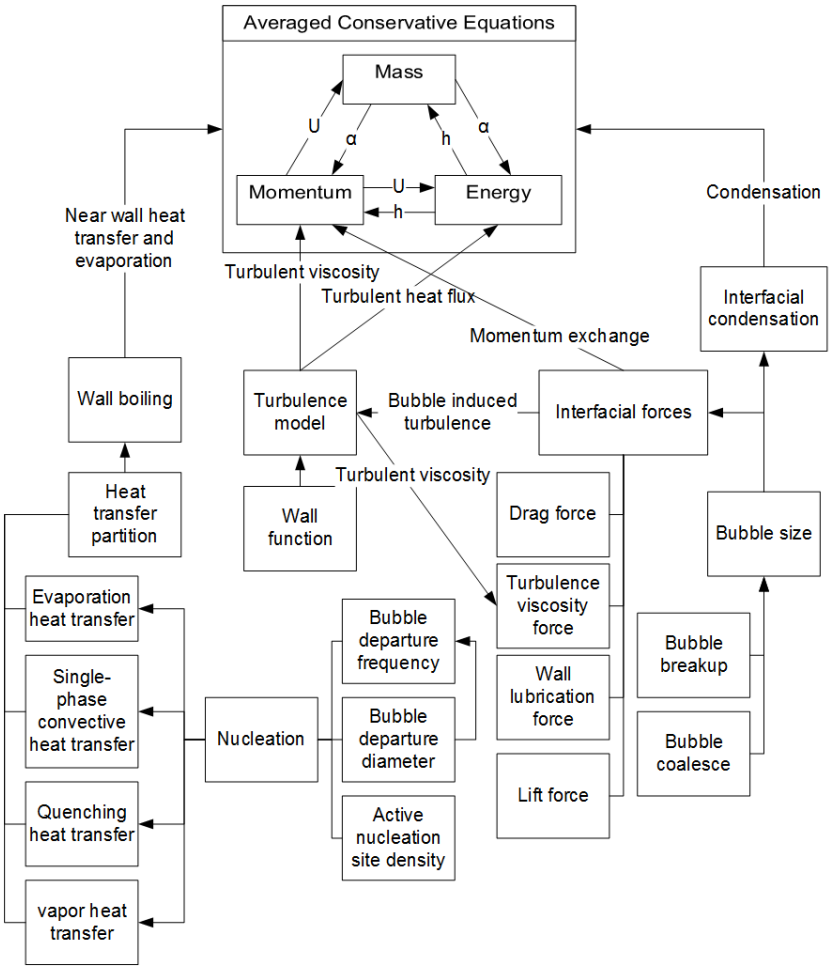

Figure 2. Closure relation structures in a typical MCFD solver

Turbulence

The modeling of turbulence in MCFD solver is based on the Reynolds-averaged Navier–Stokes (RANS) model to obtain the turbulence viscosity v^t. This type of turbulence model, which usually comes with wall functions, such as $k-\varepsilon$ model, $k-\omega$ model etc., already has been widely applied and tested in single phase flow problems. One additional closure in MCFD is to introduce a term that takes into account the bubble/droplet induced turbulence, such as the work by (Sato and Sekoguchi,1975) and (Feng and Bolotnov,2017). In most practices, only the turbulence of continuous phase - i.e. liquid phase in bubbly flow, vapor phase in droplet flow - is modeled in this way, while the turbulent viscosity of dispersed phase is assumed to be linearly dependent on the v^t of continuous phase with a turbulence response coefficient C_t.

Interfacial momentum closure relations

The interfacial momentum exchange between two phases is represented by different types of interfacial forces. For a typical MCFD solver, five interfacial forces are modeled. The drag force is modeled to describe the resistance of relative motion between the two phases. The lift force is modeled to describe the force that exerts by continuous fluid flow past the bubble. The turbulent dispersion force is modeled to describe the effect of liquid turbulence on the bubble. The wall lubrication force is designed as an artificial force to move the bubble away from the wall to describe. The virtual mass force is modeled to describe the inertia of bubble acceleration or deceleration. Figure 3 illustrates these five interfacial forces.

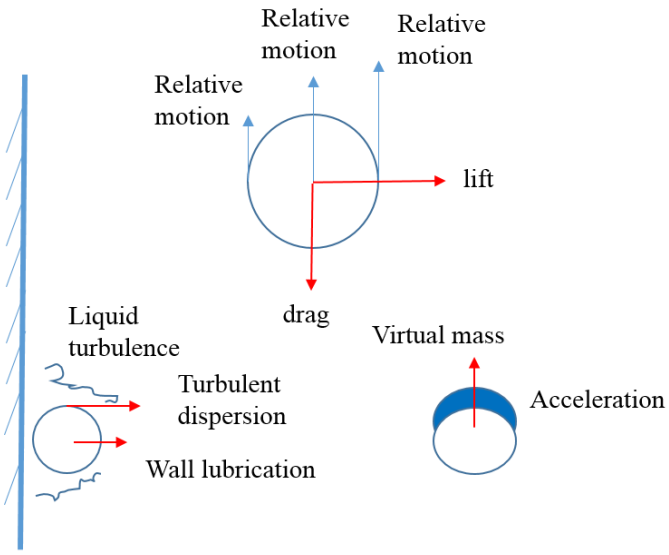

Figure 3. Schemes of interfacial forces

Table 1 summarizes the expressions of those interfacial forces. Among these interfacial forces, the form of drag force and lift force can be analytically derived; thus their expression is quite consistent among different MCFD solvers. On the other hand, the force coefficients C_d and C_l are calculated from semi-empirical correlations. For drag force, several models can be used, such as the work done by (Ishii and Zuber,1979) and (Tomiyama et al., 1998), while for lift force, the correlation developed by (Tomiyama, 1998) is widely used. It should also be noted

that in some practices, the force coefficients are also set to be constant for simplification purpose. The forms of other three forces is varied among different researchers due to the lack of solid theoretical support. Besides the expressions summarized in Table 1, there are other expressions can be used, such as the wall lubrication force model proposed by (Lubchenko et al., 2018) and turbulent dispersion force model proposed by (Burns et al., 2004).

Table 1. Expressions of interfacial forces

Force type	Expression
Drag force	$\mathbf{M}_g^D = -\frac{3}{4}\frac{C_d}{D_s}\rho_l\alpha\|\mathbf{U}_g - \mathbf{U}_l\|\left(\mathbf{U}_g - \mathbf{U}_l\right)$
Lift force	$\mathbf{M}_g^L = C_l\rho_l\alpha(\mathbf{U}_g - \mathbf{U}_l) \times (\nabla \times \mathbf{U}_g)$
Wall lubrication force (Antal et al., 1991)	$\mathbf{M}_g^{WL} = -f_{WL}(C_{wl}, y_w)\alpha\rho_l\frac{\|\mathbf{U}_r - (\mathbf{U}_r \cdot \mathbf{n}_w)\mathbf{n}_w\|^2}{D_s}\mathbf{n}_w$, $f_{WL}(C_{wl}, y_w) = \max\left(-0.2C_{wl} + (\frac{C_{wl}}{y_w})D_s, 0\right)$
Turbulent dispersion force (Gosman et al., 1992)	$\mathbf{M}_g^{TD} = -\frac{3}{4}\frac{C_D}{D_s}\frac{v_l^t}{\sigma^t Pr_l^t}\rho_l\|\mathbf{U}_g - \mathbf{U}_l\|\nabla\alpha$
Virtual mass force (Auton et al., 1988)	$\mathbf{M}_g^{VM} = -C_{vm}\rho_l\alpha\left(\frac{D\mathbf{U}_g}{Dt} - \frac{D\mathbf{U}_l}{Dt}\right)$

Interfacial mass and heat transfer closure relations

Bubbles developed from nucleation depart from the wall and join the bulk flow. In subcooled flow boiling, the bubbles become surrounded by the subcooled liquid causing vapor condensation. The interfacial mass transfer related to condensation of vapor bubbles in the bulk coolant can be described as

$$\Gamma_{\mathrm{lg}} = \frac{h_{lg}(T_{sat} - T_l)A_a}{h_{fg}}, \tag{7}$$

where h_{lg} is the heat transfer coefficient between the two phases, which can be calculated using empirical or semi-empirical correlations, representative works have been done by (Ranz and Marshall,1952) and (Chen and Mayinger,1992).

Bubble size closure relations

The size of the bubble has significant influence on the interphase exchanges of mass, energy, and momentum. Initially, the bubble size is evaluated using empirical correlation derived from subcooled flow boiling. One example of the empirical correlation, as proposed by (Anglart et al., 1997), is

$$D_s = \frac{D_{ref,1}(T_{sub} - T_{sub,2}) + D_{ref,2}(T_{sub,1} - T_{sub})}{T_{sub,1} - T_{sub,2}}, \quad (8)$$

where $T_{sub,1}, T_{sub,2}, D_{ref,1}, D_{ref,2}$ are empirical constants which have suggested values, but those values are often tuned in different applications. A more sophisticated development is to predict the bubble size distribution with the interfacial area transport equation (Hibiki and Ishii,2002). The volumetric interfacial area concentration equation can be expressed as

$$\frac{\partial(A_a)}{\partial t} + \nabla \cdot (A_a \mathbf{U}_a) = \frac{2}{3}\frac{A_a}{\alpha}\left(\frac{\partial \alpha}{\partial t} + \nabla \cdot (\alpha \mathbf{U}_a)\right) + \Phi_{\mathrm{BB}} + \Phi_{\mathrm{BC}} + \Phi_{\mathrm{NUC}}, \quad (9)$$

in which the first term on the right-hand side refers to the contribution of phase change and expansion due to pressure-density change. Here Φ_{BB}, Φ_{BC}, and Φ_{NUC} represent the source and sink term induced by breakup, coalescence, and nucleation respectively. There are several semi-empirical correlations for those terms proposed by different researchers, reprehensive works include (Yao and Morel,2004), and (Nguyen et al., 2013).

Another mechanistic approach for bubble size prediction is the multiple size group (MUSIG) model which deals with the non-uniform bubble size distribution by dividing the bubble size distribution into a finite number of groups. A more recent progress is the inhomogeneous MUSIG model by (Krepper et al., 2008) which allows each bubble group to have its own velocity.

Wall boiling closure relations

Nucleation and growth of vapor bubbles serve as a mechanism for efficient cooling of the superheated fluid layer and hence heat removal from the heated wall. The wall boiling closure relation in MCFD solver is developed to provide a consistent treatment of phenomena that govern heat transfer in boiling. The general approach is termed “heat partitioning”, which decomposes the wall heat flux into several components representing corresponding heat transfer mechanisms. The wall boiling model was first introduced by (Kurul and Podowski,1991), which partitions the wall heat flux into three components: single phase forced convective heat transfer, quenching heat transfer, and evaporation heat transfer. This model is often called “Generation-I” model as many new refined models are developed based on it. It can be expressed as

$$q_{wall} = q_{Ev} + q_{Qu} + q_{Fc}. \quad (10)$$

The quenching heat transfer describes the heat transfer towards the liquid phase when the cool liquid replaces the detached bubbles from the wall. The quenching heat flux can be calculated with the expression proposed by (Del Valle and Kenning,1985):

$$q_{Qu} = A_b \frac{2}{\sqrt{\pi}} f \sqrt{t_{wait} k_l \rho_l c_{p,l}} (T_{sup} - T_l), \quad (11)$$

where t_{wait} is the waiting time between the bubble departure and the appearance of a new bubble at a given nucleation site, which can be modeled by different empirical correlations.

The forced convective heat transfer happens in the area where no nucleation happens. The convective heat flux can be modeled as:

$$q_{Fc} = (1 - A_b)h_l\left(T_{sup} - T_l\right), \tag{12}$$

where h_l is the convective heat transfer coefficient which is usually modeled with semi-empirical correlations that take into account the near wall turbulence.

In the boiling process, a significant proportion of heat transfer is served for evaporation. The bubbles appear and grow on the active nucleation site until departure. Therefore, the evaporation heat flux is dependent on the nucleation site densityN_a, bubble departure diameter D_d, and bubble departure frequency f_d:

$$q_{Ev} = \frac{\pi}{6} D_d^3 \rho_v f_d N_a h_{fg}. \tag{13}$$

Selected empirical correlations for those nucleation phenomena are summarized in Table 2, Table 3, and Table 4, respectively. A more comprehensive review of those empirical correlations also can be found in (Cheung et al., 2014). It should also be noted that the evaporation heat transfer also serves as a void fraction source term in the mass conservation equation.

Table 2. Selected models for nucleation site density

Model	Empirical correlation for N_a, m^{-2}	Condition
(Lemmert and Chawla,1977)	$N_a = \left(aT_{\mathrm{sup}}\right)^b$, a = 210, b = 1.805	Pool boiling
(C. H. Wang and Dhir,1993)	$N_a = 5 \times 10^{-31}(1 - cos\theta)R_c^{-6.0}$	Pool boiling, p=1bar
(Yang and Kim,1988)	$N_a = N_{avg}\phi(\beta)exp(-CR_c)$	Pool boiling
(Hibiki and Ishii,2003)	$N_a = N_{avg}\left[1 - exp\left(-\frac{\theta^2}{8\mu_{con}^2}\right)\right]\left[exp\left(\frac{\lambda' g(\rho^+)}{R_c}\right) - 1\right]$	Pool and flow boiling, p ~ [1-198] bar

Table 3. Selected models for bubble departure diameter

Model	Empirical correlation for D_d, m	Condition
(Cole and Rohsenow,1969)	$D_d = 1.5 \times 10^{-4}\sqrt{\frac{\sigma}{g\Delta\rho}}\left(\frac{\rho_l C_{pl} T_{sat}}{\rho_g h_{fg}}\right)^{5/4}$	Pool nucleate boiling
(Tolubinsky and Konstanchuk,1972)	$D_d = \min[0.06exp(-\Delta T_{sub}/45),0.14]$, mm	Subcooled flow boiling
(Kocamustafaogullari, 1983)	$D_d = 1.27 \times 10^{-3}\left(\frac{\rho_l - \rho_g}{\rho_g}\right)^{0.9} d_{ref}$	Pool and flow boiling, p ~ 1-142 bar
(Zeng et al., 1993)	Mechanistic model bubble departure/lift-off based on force balance analysis	Pool and Flow boiling

Table 4. Selected models for bubble departure frequency

Model	Empirical correlation for f, s^{-1}	Condition
(Cole, 1967)	$f_d = \sqrt{\frac{4g(\rho_l - \rho_g)}{3D_d\rho_l}}$	Pool nucleate boiling near CHF
(Kocamustafaogullari and Ishii,1995)	$f_d = \frac{1.18}{D_d}\left[\frac{\sigma g(\rho_l - \rho_g)}{\rho_l^2}\right]^{0.25}$	Subcooled _flow boiling
(Podowski et al., 1997)	Mechanistic model accounts for waiting time and bubble growth time	subcooled flow boiling

It is noted that in the "Generation-I" model, some of the important phenomena in flow boiling were not considered, such as the bubble sliding effect and the nucleation site interaction under high heat flux boiling. Some more recent efforts to resolve such issues have been made (Basu et al., 2005), (Yeoh et al., 2014), (Hoang et al., 2017), (Gilman and Baglietto,2017). The refined models resolve the underlying physics during nucleation and bubble growth. A common feature of those refined boiling models is the consideration of bubble sliding effect in flow boiling. The differences between those refined boiling models and the "Generation-I" model are summarized in Figure 4.

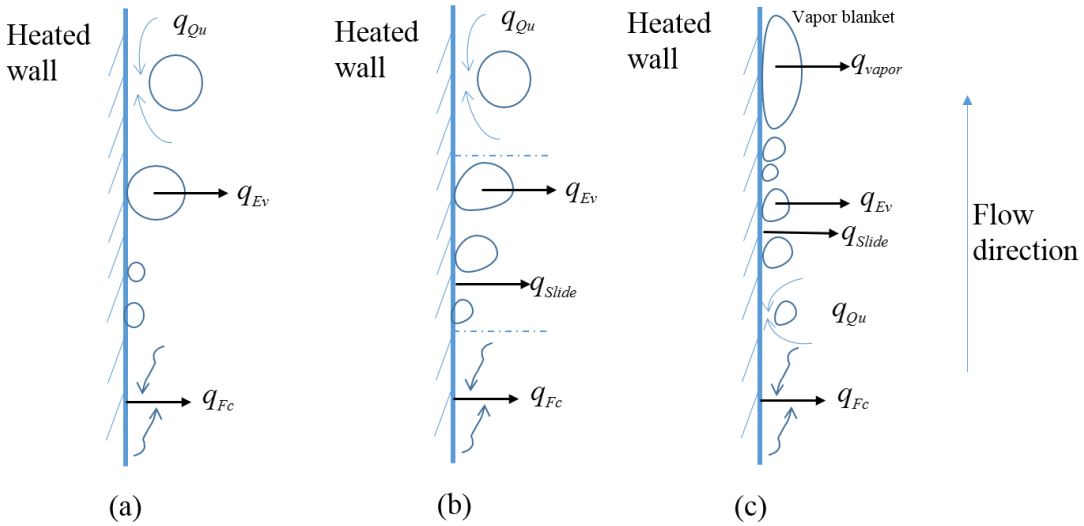

Figure 4. Illustration of heat partitioning in (a)."Generation-I" boiling model; (b).Refined boiling models; (c). Boiling model for DNB prediction

To summarize, the MCFD solver is based on a system that consists of three conservative equations and a set of closures included in the equations. The solver discretizes and numerically solves this system. The empirical parameters in the closures contribute to a major uncertainty source of the solver. Similar to the validation hierarchy, the role of closures in the system is also a reflection of the "divide-and-conquer" philosophy that decompose a complex system into

several sub-phenomena and modeled them with closures separately. Effective as this approach is, it could underestimate or even ignore the interaction between different sub-phenomena. A consequence of this approach is the non-negligible model form uncertainty. In this sense, both the model parameter uncertainty and the model form uncertainty needs to be considered in the VUQ of MCFD solver.

4. VUQ Framework for MCFD solvers

As discussed in Section2.3, a validation framework for CFD based on the phenomena decomposition has been proposed for two decades (AIAA, 1998). Although the framework has detailed guidance and solid theoretical background, limited validation practice has been conducted based on it. The major reason is the strict requirement of the validation data support, which current traditional experiments often cannot provide. Instead, a more convenient and straightforward validation paradigm has been adopted. This approach first identifies a set of closure relations that are considered to be important to the system of interest, then conduct parameter tuning on the closure relation based on available separate-effect test (SET) data. The tuned closure relations are then employed in the solver to obtain the QoIs and compare with the integrated-effect test (IET) data. This approach can produce reasonably good results with a limited data support. On the other hand, there are some shortcomings for this approach. The parameter tuning heavily depends on the researcher's experience and is generally providing *ad hoc* result. Also, the obtained results cannot be updated with newly available data. Moreover, the possible interactions between the closure relations are neglected through this approach.

To overcome the shortcoming of the aforementioned traditional validation paradigm and to avoid the strict requirement for validation data, a new validation framework based on the idea of total data-model integration (TDMI) is proposed in this paper. The TDMI approach treats closure relations, solver, and data in an integrated manner within the Bayesian framework. Taking the MCFD solver as an example, for a given solver, the closure relation structure and the corresponding phenomena decomposition are already fixed. When using TDMI approach, the solver with its closures are treated as an integrated mathematical model which is like a "black-box" computational model with parameters serving as inputs and QoIs as outputs. This "black-box", along with available data, are employed in the Bayesian framework to quantify the uncertainty of both the influential parameters and the QoIs. This approach ensures the possible interaction between different closure relations to be considered, and the results can be automatically updated with newly available data. Another advantage of TDMI is its flexibility with data. It is capable to simultaneously take into account multiple QoIs measured under different conditions. Moreover, it can provide a reasonable VUQ result with limited available data, and can also give a more accurate result with better data support. The VUQ relationship between MCFD solver and data under TDMI approach is illustrated in Figure 5.

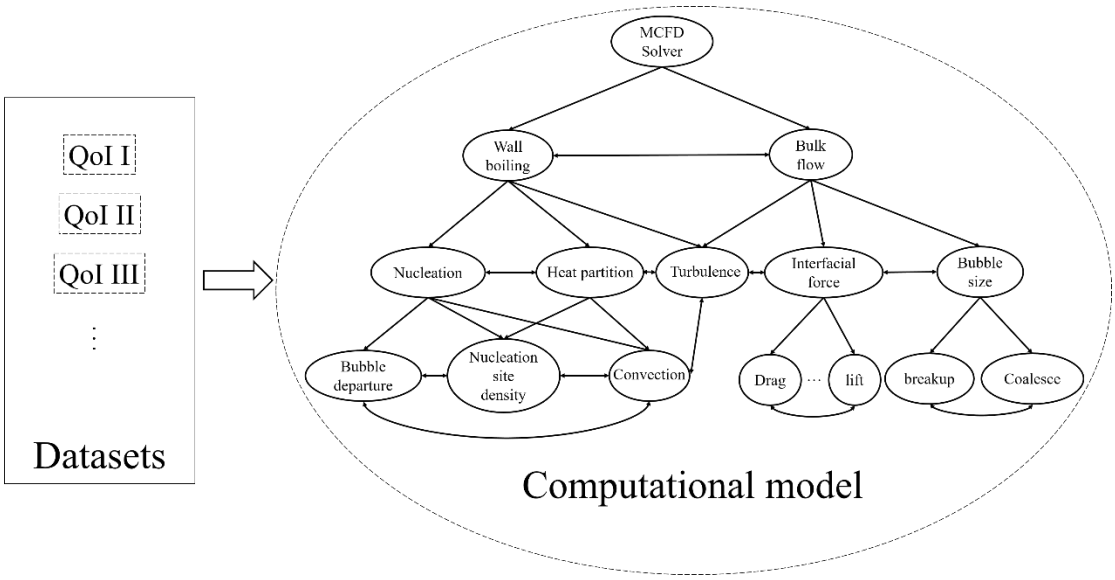

Figure 5. VUQ relationship of MCFD solver, closure relations, and data under TDMI approach

It is obvious that in the TDMI approach, the validation is tightly coupled with the UQ process. The Bayesian method serves as the core method in this approach. The TDMI with the Bayesian method has been firstly demonstrated in (Bui et al., 2013) for the two-phase drift-flux model with synthetic data. The comparison between the traditional validation and TDMI based VUQ is illustrated in Figure 6.

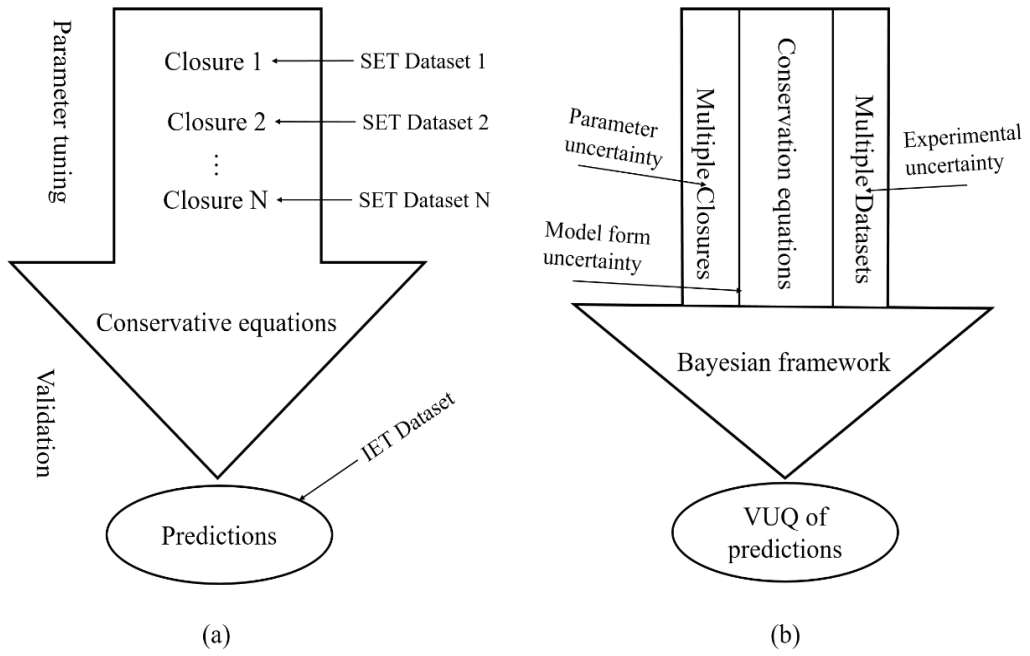

Figure 6. Two different validation paradigms: (a) Traditional validation; (b)VUQ based on total data-model integration

The VUQ framework is proposed as a six-step procedure. It is formed in a modular manner, which means each step of the workflow can be treated independently and the specific method applied in a step will not influence the following steps. For example, for the surrogate construction (step 2), one can choose a method that fits their problem best, such as Gaussian process, Stochastic collocation or support vector machine, and this choice will not influence the further steps of the work. Moreover, for each step, the non-intrusive method can be used which ensures the extendibility of the framework to different MCFD solvers. The workflow of the framework is summarized in Figure 7.

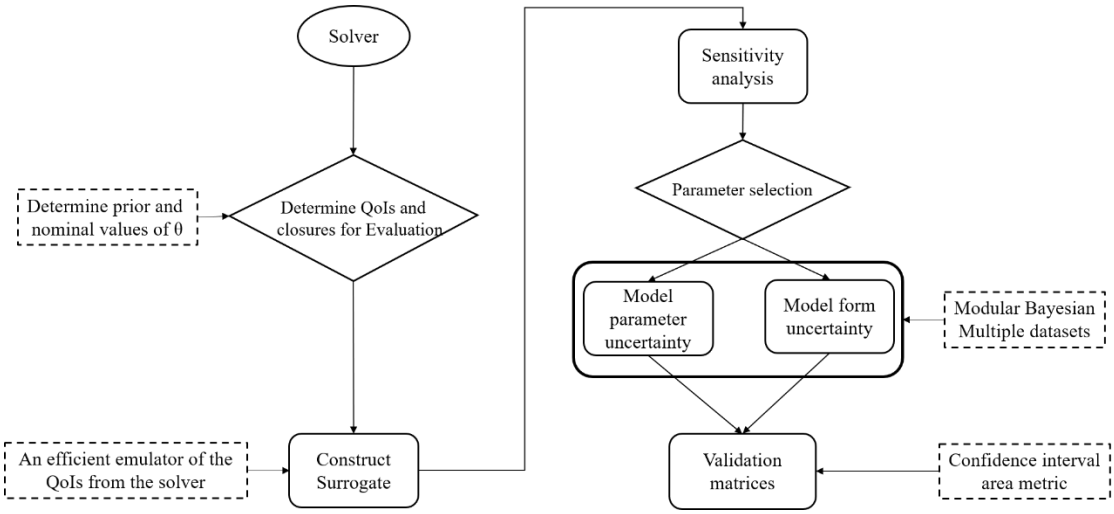

Figure 7. Workflow of the proposed VUQ framework

As discussed in the introduction, the ultimate goal of this VUQ framework is to answer the question: How to evaluate if a MCFD adequately represents the underlying physics of a multiphase system of interest? In this section, this question is further decomposed into several smaller questions and is discussed in detail:

- How to choose relevant closure relations for a given scenario (section 4.1)
- How to build an accurate and efficient surrogate model for statistical inference? (section 4.2)
- How to identify influential and identifiable parameters (section 4.3 and section 4.4)
- How to quantify the model parameter uncertainty with the given available datasets? (section 4.5)
- How to evaluate the model form uncertainty which should be independent of parameters? (section 4.5)
- How to quantify the uncertainties of all the QoIs in a simultaneous manner? (section 4.5)
- How to build confidence in applying VUQ results on an untested condition? (section 4.5)?
- How to quantitatively validate the QoIs' full distribution against experimental measurements (section 4.6)?

4.1 First step: solver evaluation and data collection

The MCFD solver deals with many different scenarios related to multiphase flow, from adiabatic bubbly flow to subcooled boiling flow. For different problems, the closure relations used for simulation could be different and the Quantities of Interest (QoIs) would also vary. In this sense, the initial step in the procedure is evaluating the solver based on scenarios and collecting relevant experimental data to support the VUQ process.

Based on the studied scenario, several items should be addressed in this step:

- Evaluation of QoIs
- Collection of available experimental datasets
- Evaluation of closure relations
- Evaluation of input parameters

The QoIs of an MCFD simulation is scenario dependent and needs to be specified in the first place. For example, for boiling flow simulation, the wall superheat is considered as a QoI since it closely relates to safety, while the heat partitions are also QoIs since it relates to the heat transfer efficiency. For adiabatic bubbly flow, the interface distribution (characterized by void fraction) and the phasic flow field are QoIs. Once the QoIs for the given scenario is determined, the experimental measurement for the QoIs should be collected. For most cases, the resolution of the experimental measurement is coarse than the simulation results whose resolution can be easily controlled through mesh setup. The proposed VUQ framework can deal with such limited data availability issue within the Bayesian framework. On the other hand, the VUQ results would be more accurate with the support of detailed measurement from validation experiments. Also, the framework takes measurements from different conditions (e.g. different mass flow rate, heat flux, etc.) for the VUQ work simultaneously. This would generate robust VUQ results that can be extended to untested conditions.

As discuss in section 2, there are many closure relations of different categories in a MCFD solver. Some of the closure relations have very limited influence on certain QoIs or are even not activated in certain scenarios. Thus, it is impractical and unnecessary to evaluate the parameters of all closure relations for a given scenario. The evaluation of closure relations aims to identify closure relations that are relevant to the QoIs of a scenario. Once the relevant closure relation is evaluated, the uncertainties of the corresponding parameters are then inversely quantified through the Bayesian inference. To perform Bayesian inference, the empirical parameters are treated as random variables with given prior distribution that base on “expert judgment”.

4.2 Second step: Surrogate construction

The VUQ process requires many solver evaluations, considering the relative expensiveness of running a MCFD simulation, a surrogate model, also known as response surface model or emulator, is a necessary. In this step, a surrogate model is constructed based on the outputs of a limited number of runs of the original solver.

In some research area, the parameter number of a model can be very huge, for this type of model, the usual procedure is to do a simplified sensitivity analysis and parameter selection first to reduce the dimensionality of parameter space, then construct the surrogate on the

reduced parameter space (Smith, 2014). For MCFD solver, the parameter size is not that huge compared to these problems. Thus in this framework, the surrogate is constructed with all parameters relevant to a certain scenario, then comprehensive sensitivity analysis and parameter selection are performed based on the surrogate.

There are multiple statistical and numerical methods that can be used for constructing a surrogate model. Each has various applications, such as polynomial response surface (Hosder et al., 2001), stochastic collocation (Wu et al., 2017), and Gaussian Process (Constantine et al., 2014), etc. In this work, we chose the Gaussian Process (GP) regression for surrogate construction, which has been widely used in the area of data-driven modeling and optimization. The only assumption for GP model is the QoIs are smooth over the whole input domain, which is generally valid for the considered problems.

The general form of a GP model can be expressed as

$$y^M(\mathbf{q},\boldsymbol{\beta}) = \sum_{i=1}^{m} h_i(\mathbf{q})^T \beta_i + \mathbf{f}(\mathbf{q}) = \mathbf{h}(\mathbf{q})^T \boldsymbol{\beta} + Z(\mathbf{q}), \tag{14}$$

where $\mathbf{q} = [\boldsymbol{q_1}, \boldsymbol{q_2}, \ldots, \boldsymbol{q_p}]$ is the p input variables, which can be empirical parameters or boundary conditions and $\boldsymbol{y^M}(\mathbf{q})$ is the model output with the given input. The first term on the right side is a deterministic trend function, which is the product of regression coefficients $\boldsymbol{\beta}=[\boldsymbol{\beta_1}, \boldsymbol{\beta_2}, \ldots, \boldsymbol{\beta_m}]$ and the basis function $\mathbf{h}(\mathbf{q}) = [\boldsymbol{h_1}(\mathbf{q}), \boldsymbol{h_2}(\mathbf{q}), \ldots, \boldsymbol{h_m}(\mathbf{q})]$, which has known form, usually set to be a constant or polynomial function. The second term $Z(\mathbf{q})$ is a GP error model with zero mean, variance σ^2 and non-zero covariance $\mathbf{cov}[\boldsymbol{Z}(\mathbf{q^1}), \boldsymbol{Z}(\mathbf{q^2})]$, which can be modeled as

$$\mathrm{cov}\left[Z(\mathbf{q}^{(i)}), Z(\mathbf{q}^{(j)})\right] = \sigma^2 K(\mathbf{q}^{(i)}, \mathbf{q}^{(j)}), \tag{15}$$

where $K(\mathbf{q}^{(i)}, \mathbf{q}^{(j)})$ is called kernel function, which is usually chosen to be a function of the distance between the two input vectors. This functional form ensures that two inputs with close distance will produce outputs that are also close together. Since not all input variables are equally important to the output, it is natural to introduce weighting factors for each input variable in the kernel. There are many forms of kernel functions, an example is the powered-exponential kernel

$$K(\mathbf{q}^{(i)}, \mathbf{q}^{(j)}) = \exp\left(-\sum_{k=1}^{p} \omega_k \left| q_k^{(i)} - q_k^{(j)} \right|^{\gamma_k} \right), \tag{16}$$

where ω_k is the weighting factors, and γ_k is termed "roughness factors", which influence the smoothness of the kernel function.

The two vectors ω and γ in equation (3), along with variance σ^2 are called hyperparameters of the GP model. The values of hyperparameters can be estimated by several methods such as Maximum Likelihood Estimation (MLE) or Bayesian inference.

As noted, a GP model needs a limited number of runs from original solver before it can be used to do prediction. Suppose N simulations of MCFD solvers are performed, the following matrices and vector are calculated:

Basis function:

$$\mathbf{H}=[\boldsymbol{h}(\mathbf{q}^1),\boldsymbol{h}(\mathbf{q}^2),\ldots,\boldsymbol{h}(\mathbf{q}^N)]=\begin{pmatrix} h_1(\mathbf{q}^1) & \ldots & h_1(\mathbf{q}^N) \\ \vdots & \ddots & \vdots \\ h_m(\mathbf{q}^1) & \cdots & h_m(\mathbf{q}^N) \end{pmatrix} \tag{17}$$

Kernel function:

$$\mathbf{K}=\begin{pmatrix} K(\mathbf{q}^{(1)},\mathbf{q}^{(1)}) & \ldots & K(\mathbf{q}^{(1)},\mathbf{q}^{(N)}) \\ \vdots & \ddots & \vdots \\ K(\mathbf{q}^{(N)},\mathbf{q}^{(1)}) & \cdots & K(\mathbf{q}^{(N)},\mathbf{q}^{(N)}) \end{pmatrix} \tag{18}$$

Output QoI:

$$\mathbf{y}^M = [y^M(\mathbf{q}^{(1)}), y^M(\mathbf{q}^{(2)}),\ldots, y^M(\mathbf{q}^{(N)})] \tag{19}$$

The regression coefficients $\boldsymbol{\beta}$ can be obtained through least-square estimate

$$\widehat{\boldsymbol{\beta}}=(\mathbf{H}^{\mathbf{T}}\mathbf{R}^{-1}\mathbf{H})^{-1}\mathbf{H}^{\mathbf{T}}\boldsymbol{K}^{-1}\mathbf{y}^{\mathrm{M}} \tag{20}$$

Thus, for a new unknown input $\boldsymbol{q}^*$, the GP model can give following prediction:

$$\hat{y}^M(\mathbf{q}^*) = \mathbf{h}(\mathbf{q}^*)\widehat{\boldsymbol{\beta}} + {K^*}^T\boldsymbol{K}^{-1}\left(\mathbf{y}^M - \mathbf{H}\widehat{\boldsymbol{\beta}}\right), \tag{21}$$

where

$$\mathrm{K}^*=\sigma^2[\mathrm{K}(\mathbf{q}^*,\mathbf{q}^{(1)}),\mathrm{K}(\mathbf{q}^*,\mathbf{q}^{(2)}),\ldots,\mathrm{K}(\mathbf{q}^*,\mathbf{q}^{(\mathrm{N})})]\,. \tag{22}$$

In addition, the GP model also give the variance of the predictor, which can be expressed as

$$\mathrm{Var}[(\hat{y}^M)] = \sigma^2\left[1-\begin{pmatrix}\mathbf{h}^{\boldsymbol{T}}(\mathbf{q}^*) & K^{*T}\end{pmatrix}\begin{pmatrix}0 & \mathbf{H}^T \\ \mathbf{H} & \mathbf{R}\end{pmatrix}^{-1}\begin{pmatrix}\mathbf{h}^{\boldsymbol{T}}(\mathbf{q}^*) \\ K^{*T}\end{pmatrix}\right]. \tag{23}$$

The accuracy of GP model in predicting the QoI with untried inputs can be evaluated through the cross-validation method. The details will be discussed in the specific applications detailed in the Part II paper.

For many cases, such as bubbly flow problem, the output QoI from MCFD solver is not only a function of boundary condition and empirical parameters but also a function of locations. Thus for even one single QoI, the output is a vector, with the size of the vector depending on the mesh setup. The straightforward approach is to train a GP model for every element of the vector respectively. This approach, however, is too cumbersome and totally ignores the spatial correlation between those outputs. The dimension reduction method Principal Component Analysis (PCA) can be applied to resolve this issue, with details in Appendix. A.

4.3 Third step: Sensitivity Analysis (SA)

Once the surrogate model for the MCFD solver is constructed, Sensitivity Analysis (SA) regarding the empirical parameters would be performed based on it. The general objective of

SA is to quantify the individual parameter's contribution towards the QoIs and determine how variations in parameters affect the QoIs.

In this framework, the Global SA (GSA) is conducted which considers the QoI uncertainties due to combinations of parameters throughout the whole admissible input space. It should also be noted that when conducting SA, the prior distributions and nominal values of all parameters are already determined in Step 1. In the following analysis, the input variables $\boldsymbol{q}$ used in constructing GP model are further characterized by parameters $\boldsymbol{\theta}$ (suppose have p dimensions) and condition variable $\boldsymbol{v}$ (such as mass flow rate, wall heat flux, etc.) and spatial dependent variable $\boldsymbol{x}$, so that $\mathbf{y}^M(\mathbf{q})$ is expressed as $\mathbf{y}^M(x, \mathbf{v}, \theta)$. There are two different methods for GSA: the Morris screening method and the Sobol indices method.

Morris Screening method

Morris Screening method evaluates local sensitivity approximations, termed elementary effects, over the input space. Morris Screening method can rank parameters according to their importance, but cannot quantify how much one parameter is more important to another. The major advantage of Morris Screening is its low computational cost.

Morris Screening is based on the linearization of the model. To construct the elementary effect, one partitions [0,1] into l levels. Thus the elementary effect associated with the i^{th} input can be calculated as

$$d_i(\boldsymbol{\theta}) = \frac{\int y^M\left(x, \mathbf{v}, \left[\theta_1, \dots, \theta_{i-1}, \theta_i + \Delta, \theta_{i+1}, \dots \theta_p\right]\right)dx - \int y^M(x, \mathbf{v}, \boldsymbol{\theta})dx}{\Delta}, \quad (24)$$

which means the QoIs are integrated over the whole input condition space for evaluation. The step size Δ is chosen from the set

$$\Delta \in \left\{\frac{1}{l-1}, \dots, 1 - \frac{1}{l-1}\right\} \quad (25)$$

For r sample points, the sensitivity measurement for x_i can be represented by the sampling mean μ_i, standard deviation σ_i^2, and mean of absolute values μ_i^*, which can be calculated respectively.

$$\mu_i^* = \frac{1}{r}\sum_{j=1}^{r} |d_i^j(\mathbf{q})| \quad (26)$$

$$\mu_i = \frac{1}{r}\sum_{j=1}^{r} d_i^j(\mathbf{q}) \quad (27)$$

$$\sigma_i^2 = \frac{1}{r-1}\sum_{j=1}^{r} \left(d_i^j(\mathbf{q}) - \mu_i\right)^2 \quad (28)$$

The mean represents the effect of the specific parameter on the output, while the variance represents the combined effects of the input parameters due to nonlinearities or interactions with other inputs. The obtained μ^* and σ can help ranking the parameters by the relative order of importance. If the value of sigma is high compared to mu (same order of magnitude), a non-linear influence and/or interactions with other parameters are detected. This measure is however only qualitative.

Variance based method: Sobol indices

Variance-based methods decompose the output variance into contributions of the input variances, in this method, the importance of parameter can be quantitatively evaluated. The Sobol indices method is one of the most widely used variance based method on GSA. In here the basic idea of Sobol indices is discussed, assuming the parameters are independent and uniformly distributed on [0,1]. A more general situation is discussed in (Smith, 2014).

A general computational model $y^M(\boldsymbol{q})$ can be expressed with second-order Sobol expansion:

$$y^M(\boldsymbol{q}) = f_0 + \sum_{i=1}^{p} f_i(q_i) + \sum_{1\le i<j\le p} f_{ij}(q_i, q_j)\,, \tag{29}$$

where the zeroth-, first-, and second-order terms on the right hand side can be expressed as

$$\begin{aligned} f_0 &= \int_{\Gamma^p} y^M(\boldsymbol{q}) d\boldsymbol{q}\,, \\ f_i(q_i) &= \int_{\Gamma^{p-1}} y^M(\boldsymbol{q}) d\boldsymbol{q}_{\sim i} - f_0\,, \\ f_{ij}(q_i, q_j) &= \int_{\Gamma^{p-2}} y^M(\boldsymbol{q}) d\boldsymbol{q}_{\sim i} - f_i(q_i) - f_j(q_j) - f_0\,, \end{aligned} \tag{30}$$

where $\Gamma^p = [0,1]^p$. The notation $\boldsymbol{q}_{\sim i}$ denotes the vector having all the components of $\boldsymbol{q}$ except i^{th} element.

The total variance D of the model prediction y^M is

$$D = \mathrm{var}(y^M) = \int_{\Gamma^p} {y^M}^2(\boldsymbol{q}) d\boldsymbol{q} - f_0^2\,, \tag{31}$$

which can be furtuer expressed as

$$D = \sum_i D_i + \sum_{1\le i<j\le p} D_{ij}\,, \tag{32}$$

where D_i and D_{ij} are two partial variances can be expressed as

$$\begin{aligned} D_i &= \int_0^1 f_i^2(q_i) dq_i \\ D_{ij} &= \int_0^1 f_{ij}^2(q_i, q_j) dq_i \end{aligned}\,. \tag{33}$$

The Sobol indices are defined to be

$$S_i = \frac{D_i}{D},\ S_{ij} = \frac{D_{ij}}{D},\ i, j = 1, \ldots, p \tag{34}$$

By definition, those indices satisfy

$$\sum_{i=1}^{p} S_i + \sum_{1 \le i < j \le p} S_{ij} = 1\,, \tag{35}$$

where S_i is termed the *first-order sensitivity indices*, large value of S_i indicate strong influence of the corresponding parameter on the model prediction. S_{ij} measures the influence of interaction between two corresponding parameters. Based on this two terms, the *total sensitivity indices* can be calculated to quantify the total effect of the corresponding parameter on model prediction

$$S_{T_i} = S_i + \sum_{j=1}^{p} S_{ij} \tag{36}$$

In practice, both the first-order indices and total sensitivity indices are considered using this method. The detailed algorithm to calculate the Sobol indices is included in Appendix. B.

4.4 Forth step: Parameter selection

For a complex system such as the MCFD solver, many empirical parameters exist in the closure relations, and the parameter identifiability arises as a major issue for conducting Bayesian inference. This issue stems from the fact that with a limited number of datasets, there could exist different values of parameters that produce very similar results and fit the data equally well. The convergence of Bayesian inference would face difficulty with non-identifiable parameter exists, unless good prior distributions are provided. Moreover, for engineering applications, the VUQ results should provide guidance for setting up parameters for future cases, thus a subset of parameters quantified with small uncertainties is more helpful for engineering simulation compared to the complete set of parameters quantified with large uncertainties. In this sense, it is desired to find a subset of parameters that not only can be identified using measured data but also with high sensitivity so that the Bayesian inference would give smaller posterior uncertainties of parameters. In this sense, the parameter selection is closely related to SA. The objective of this step is to perform SA and select a subset of parameters based on SA for the Bayesian inference in next step.

It is natural to select parameters based on the GSA results. The general idea is to select parameters with high impact to the QoIs which are identifiable in the sense that they can be uniquely determined by the data. However, even two highly influential parameters cannot guarantee that they are mutually identifiable. A most straightforward example is $y = a + b$, where a and b are of equal importance, but they are not identifiable with each other. Thus based on the GSA results, the parameter selection is still an *ad hoc* solution which requires trial-and-error.

An algorithm for parameter selection has been developed by (Banks et al., 2013), which is based on the local sensitivity matrix, instead of the GSA results. The selection scores of different combinations of parameters can be obtained. The detailed implementation of the algorithm is given in Appendix. C.

Compared to the trial-and-error approach based on GSA, this algorithm also has its drawbacks. Since the algorithm is based on the nominal parameter value $\boldsymbol{\theta_0}$, it does not fully explore the

whole parameter space. In this sense, there is a possibility that such selection may be misleading if the parameter posterior distribution deviates significantly to the nominal value. Moreover, since there are multiple QoIs taken into consideration, the "optimal" parameter subset for different QoI could be different. In this sense, subjectivity cannot be avoided in the parameter selection. To sum up, the parameter selection process introduced in this work can be regarded as an "expert judgment informed by sensitivity analysis" procedure. In the following Bayesian inference step, only the selected parameters are treated as random variables while other parameters are fixed at their nominal values.

4.5 Fifth step: UQ with Bayesian inference

For a general computational model, the relationship between the outputs and experimental measurements can be expressed as

$$\mathbf{y}^E(\mathbf{x},\mathbf{v}) = \mathbf{y}^M(\mathbf{x},\mathbf{v},\boldsymbol{\theta}) + \delta(\mathbf{x},\mathbf{v}) + \varepsilon(\mathbf{x},\mathbf{v}), \tag{37}$$

where $\mathbf{y}^E(\mathbf{x},\mathbf{v})$ is the experimental measurement, $\mathbf{y}^M(\mathbf{x},\mathbf{v},\boldsymbol{\theta})$is the model prediction, $\delta(\mathbf{x},\mathbf{v})$ is the model form uncertainty, which is usually caused by missing physics, simplified assumptions or numerical approximations in the model, $\varepsilon(\mathbf{x},\mathbf{v})$ is the measurement uncertainty which is assumed to be i.i.d (independent and identically distributed) normal distributions with zero means and know variance σ^2 in this work:

$$\varepsilon(\mathbf{x},\mathbf{v}) \sim N(0,\sigma^2\mathbf{I}) \tag{38}$$

The goal in inverse UQ process is to evaluate the uncertainty of the parameter based on the data. In the framework of Bayesian inference, which treats the parameter as random variables, the prior knowledge for the parameter is also considered. The prior knowledge usually comes from previous simulations, other experimental observations or purely expert opinion. The Bayes formula is the foundation of Bayesian inference:

$$p(\boldsymbol{\theta}|\mathbf{y}^E) = \frac{p(\mathbf{y}^E|\boldsymbol{\theta})p_0(\boldsymbol{\theta})}{p(\mathbf{y}^E)} \propto p(\mathbf{y}^E|\boldsymbol{\theta})p_0(\boldsymbol{\theta}), \tag{39}$$

where $p(\mathbf{y}^E|\boldsymbol{\theta})$is the likelihood function, and $p_0(\boldsymbol{\theta})$is the prior distribution of $\boldsymbol{\theta}$. Under the assumption that $\varepsilon(\mathbf{x},\mathbf{v}) \sim N(0,\sigma^2\mathbf{I})$, the likelihood function has the form

$$L(\boldsymbol{\theta}|\mathbf{y}^E) = \frac{1}{(2\pi\sigma^2)^{n/2}} \exp\left(-\sum_{i=1}^{n} \frac{\left(y^E(x_i,\mathbf{v}) - y^M(x_i,\mathbf{v},\boldsymbol{\theta}) - \delta(x_i,\mathbf{v})\right)^2}{2\sigma^2} \right), \tag{40}$$

If we only care about the point estimate of the parameter, the Maximum a posteriori (MAP) method can be applied. If the prior is set to be uniform, the MAP can be obtained by maximizing Eq.(40). Due to the monotonicity of the logarithm function, it is numerically advantageous to maximize the log-likelihood function, which can be expressed as

$$l(\boldsymbol{\theta}|\mathbf{y}^E) = -\frac{n}{2}\ln(2\pi) - \frac{n}{2}\ln(\sigma^2) - \sum_{i=1}^{n} \frac{(y^E(x_i,\mathbf{v}) - y^M(x_i,\mathbf{v},\boldsymbol{\theta}) - \delta(x_i,\mathbf{v}))^2}{2\sigma^2}. \quad (41)$$

On the other hand, the full distribution of the posterior is more difficult to obtain. For most cases, the posteriori cannot be direct calculated. Based on the likelihood function and prior distribution, the posterior distribution of the parameter can be drawn through the Markov Chain Monte Carlo (MCMC) sampling. However, a still unresolved issue is the unknown term model form uncertainty $\delta(\mathbf{x},\mathbf{v})$. The investigation of the model form uncertainty is an active topic in the statistics community. The intrinsic difficulty for this problem is the confounding between model form uncertainty $\delta(\mathbf{x},\mathbf{v})$ and the parameter $\boldsymbol{\theta}$. In other words, if discrepancy is observed between the model prediction and experimental data, there is no way to distinguish if this is caused by mode form uncertainty or a "poorly" chosen model parameter without given any prior knowledge.

The data driven approach, which use a Gaussian process to evaluate the model form uncertainty term $\delta(\mathbf{x},\mathbf{v})$, has been widely used since proposed by (Kennedy and O'Hagan,2001). This data driven approach can be further divided into two types. One approach is often called "full Bayesian" (Higdon et al., 2008), which treats the hyperparameters of the GP for $\delta(\mathbf{x},\mathbf{v})$ as random variables with specified prioris and infers their posterior distributions in the same MCMC process for the inference of empirical parameters. For problems with rich data sources, such as weather forecasting, those hyperparameters can have noninformative prior in the Bayesian inference. For other cases where the data sample is not that rich, tight priors need to be assigned to those hyperparameters. Such prior setup reflect the assumption that one has good understanding on the model form uncertainty terms. The other approach is termed "modular Bayesian" approach (F. Liu et al., 2008), which firstly evaluate the hyperparameters in $\delta(\mathbf{x},\mathbf{v})$ with the point estimate method such as MLE to get a fixed form of $\delta(\mathbf{x},\mathbf{v})$. Then performs MCMC for only empirical parameters with the $\delta(\mathbf{x},\mathbf{v})$ term included in the process. The "modular Bayesian" approach doesn't require a rich data support of strong prior for the hyperparameters and is thus considered to be a more realistic and feasible approach compared to "full Bayesian". In this work, the "modular Bayesian" approach is adopted for the treatment of $\delta(\mathbf{x},\mathbf{v})$ which can be summarized in following steps:

1. Split the available datasets into three groups: one for parameter inverse UQ, one for model form uncertainty evaluation, one for testing.
2. The model form uncertainty term $\delta(\mathbf{x},\mathbf{v})$ is modeled by GP (noted that this GP model is independent with the surrogate model) based on the training datasets: $y^E(\mathbf{x},\mathbf{v}) - y^M(\mathbf{x},\mathbf{v},\boldsymbol{\theta}_0)$ with all the parameter fixed at their nominal values. The hyperparameters are obtained using MLE method and keep fixed.
3. obtain the posterior uncertainty distributions of parameters using Bayesian inference. When performing Bayesian inference on the parameters, $\delta(\mathbf{x},\mathbf{v})$ is introduced in as shown in Eq.(37).

4. Propagate the uncertainty of the parameters through the solver (which is represented by the surrogate model) to obtain the uncertainty of the QoIs.

The procedure is summarized in Figure 8.

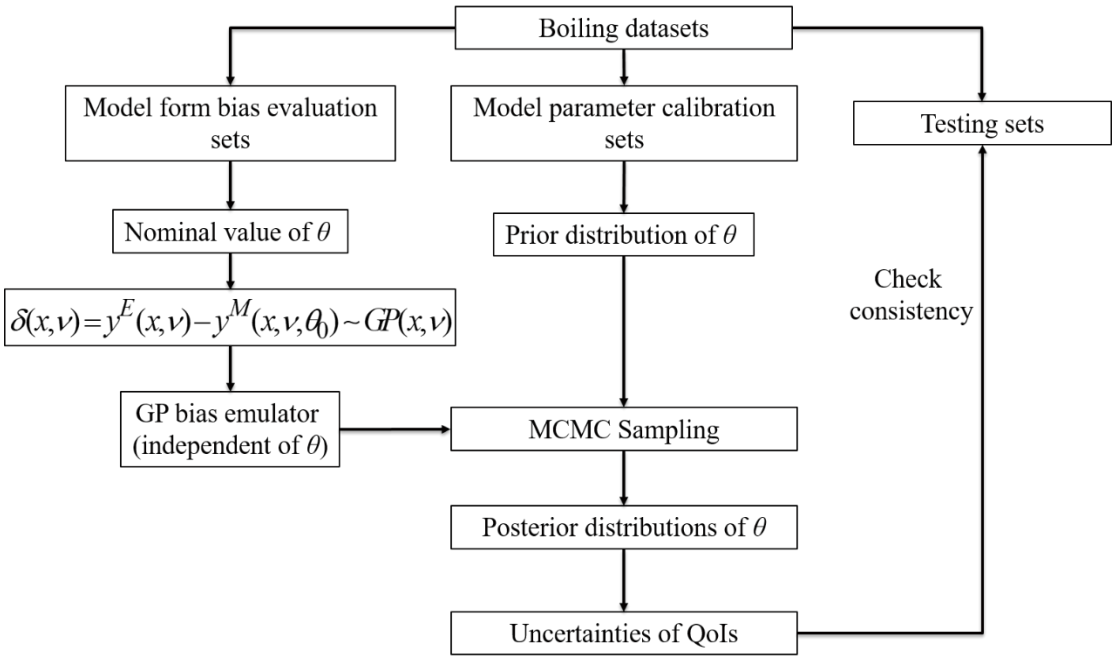

Figure 8. Evaluation of model form uncertainty and model parameter uncertainty

The general idea of MCMC is to construct Markov chains that converge to the posterior parameter distributions. For a given parameter, it is proved that the stationary distribution of the Markov chains is the posterior density. There are multiple algorithms for MCMC sampling; in this work, the Delayed Rejection Adaptive Metropolis (DRAM) algorithm (Haario et al., 2006) is used. Once the posterior distributions of parameters are obtained, the forward UQ can be applied to obtain the distributions of QoIs based on the surrogate model.

4.6 Sixth step: Validation metrics

Once the uncertainties of QoIs are obtained, the last step of the framework is to quantitatively evaluate the agreement between QoIs predicted by solver and the experimental measurements. This is done by calculating the validation metrics. In this practice, two types of validation metric are calculated.

The first type is Confidence interval. For experimental data obtained from literature, the detailed measurement information is usually not available. Thus the uncertainty of experimental data is assumed to follow normal distribution instead of t-distribution. The Eq.(1) based on t-distribution is modified to following

$$\left(\tilde{\mathbf{E}} - z_{\alpha/2} \cdot \sigma, \tilde{\mathbf{E}} + z_{\alpha/2} \cdot \sigma\right) \tag{42}$$

where σ is the standard deviation of the experimental data, and $z_{\alpha/2}$ is the 1-α/2 quantile of the statistic distribution of the experimental data. The obtained CI can be interpreted as "we have $(1-\alpha)\times 100\%$ confidence that the true discrepancy between model and observed data is within the interval".

The second type applied in the framework is the area metric. In this type of validation metric, both the experimental data and model predicted QoIs are treated as random variables, whose probability distribution is their uncertainty distribution. The area metric measures the area between the two Cumulative Distribution Functions (CDFs), which can be calculated with Eq.(3).

The validation metrics are calculated for both pure model predictions and model prediction plus model form uncertainty. The discrepancy between these two different calculations reflects the closure relations' ability to capture the corresponding physical process in the given application domain. An example of the two different validation metrics is provided in Figure 9.

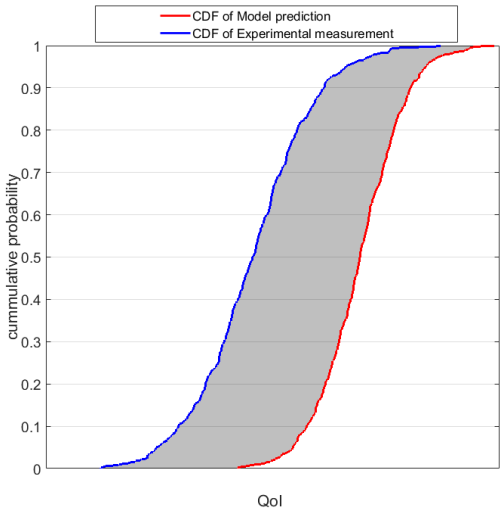

Figure 9. Example of area metric

5. Conclusions

In this work, a VUQ framework designed for Eulerian-Eulerian two-fluid-model based MCFD solver is proposed. The gold of the framework is to evaluate whether the solver represents the underlying physics of a multiphase flow and boiling system of interest with acceptable accuracy. This is accomplished through a six step procedure with two major results obtained: i). quantify the uncertainties of the closure parameters and predictions of the MCFD solver; ii). evaluate the agreement between the solver predictions and the experimental measurements.

There are several advantages of the proposed framework. Firstly, it is modular and non-intrusive. This ensures the framework's flexibility for different scenarios as well as its extendibility to different MCFD solvers. Secondly, the framework also has strong flexibility with data. It is capable of simultaneously taking into account multiple QoIs measurement under different conditions. Moreover, it can provide a reasonable VUQ result with limited data availability, while providing a more accurate result with better data support. Thirdly, the TDMI treatment ensures the VUQ considers the possible closure interactions in the MCFD solver. Last, the model form uncertainty is considered which can serve as an additional correction term to the model prediction. The validation metrics differences between pure model prediction and

prediction corrected by model form uncertainty can also serve as a measure of closure relations' ability to capture the corresponding physical process in the given application domain.

There are also limitations of the framework. Firstly, the numerical error introduced by discretizing the PDEs is not considered in this framework. Rather, this part of the error is implicitly integrated into the model form uncertainty term. Secondly, additional uncertainty would be introduced by the statistical methods applied in the surrogate construction step, such as Gaussian process and dimension reduction. Such uncertainty varied through different statistical methods and is difficult to get an estimation for the whole validation domain. A more comprehensive work in future should include the verification work to take into account the numerical error and uncertainty, also with a more rigorous method to evaluate the uncertainty introduced by statistical methods.

Appendix A. Dimension reduction of model outputs based on PCA

The PCA uses an orthogonal transformation to convert a set of observations of possibly correlated variables into a set of values of linearly uncorrelated variables called principal components. The number of principal components is less than or equal to the smaller of the number of original variables or the number of observations. The Singular Value Decomposition (SVD) is a robust algorithm for PCA.

The implementation of PCA to the MCFD solver output can be summarized as several steps. Firstly, concatenate the output vectors of different QoIs to form a long vector; e.g.:

$$\mathbf{y}^M = \left[\alpha_1, \alpha_2, \ldots \alpha_d, U_{g1}, U_{g2}, \ldots U_{gd}\right]^T, \tag{43}$$

where α_{i} and U_{gi} are the void fraction and gas velocity in mesh index i, respectively. Thus the length of the output vector is $n \times d$ where n is the number of QoIs and d is the number of meshes.

Evaluate the output vector with N different MCFD simulations. Thus an output matrix $\mathbf{Y}$ with dimension $nd \times N$ can be constructed:

$$\mathbf{Y} = \left(\mathbf{y}^M(\mathbf{q}^{(1)}), \mathbf{y}^M(\mathbf{q}^{(2)}), \ldots, \mathbf{y}^M(\mathbf{q}^{(N)})\right). \tag{44}$$

Center the output matrix by subtracting the mean column vector $\bar{\mathbf{y}}^M = \frac{1}{N}\sum_{i=1}^{N} y^M(\mathbf{q}^{(i)})$ in each column to obtain $\mathbf{Y_c}$. Then Perform SVD on $\mathbf{Y_c}$:

$$\mathbf{Y_c} = \mathbf{U\Sigma V}^{\boldsymbol{T}}. \tag{45}$$

This means the centered output matrix $\mathbf{Y_c}$ can be decomposed as the products of three matrices, where $\mathbf{\Sigma}$ is a $nd \times N$ diagonal matrix whose diagonal entries are non-negative and ordered from largest to smallest, those diagonal entries are known as singular values of $\mathbf{Y_c}$ which are the root of the eigenvalues of $\mathbf{Y_c}\boldsymbol{Y_c^T}$, whereas the eigenvalues are the measure of the variances of $\mathbf{Y_c}$. $\mathbf{U}$ is a $nd \times nd$ unitary matrix, whose columns are the left-singular vectors of $\mathbf{Y_c}$ and $\mathbf{V}$ is a $N \times N$ unitary matrix whose column vectors are the right-singular vectors of $\mathbf{Y_c}$. The column vectors of $\mathbf{U}$ are called the Principal Components (PCs).

Since **U** is unitary matrix, it has the property for such manipulation:

$$\mathbf{U}^{T}\mathbf{Y}_{c} = \mathbf{U}^{T}\mathbf{U}\boldsymbol{\Sigma}\mathbf{V}^{T} = \boldsymbol{\Sigma}\mathbf{V}^{T} = \mathbf{S}\,. \tag{46}$$

This means the PCs map each row vector of $\mathbf{Y}_c$ to a new vector (the row vector in **S**) which is termed PC scores. The PC scores are the transformed representations of the original input matrix $\mathbf{Y}_c$. For most cases, the singular values of $\mathbf{Y}_c$ decrease very quickly which means the first few PCs can quantify the structures of the $\mathbf{Y}_c$. So the manipulations in Eq.(46) can be modified as:

$$\mathbf{U}^{*T}\mathbf{Y}_{c} = \mathbf{S}^{*}\,, \tag{47}$$

where $\mathbf{U}^{*}$ is a $nd \times d^{*}$ matrix with first d^{*} PCs, $\mathbf{S}^{*}$ is the corresponding $d^{*} \times N$ matrix with first d^{*} PC scores. In practice, one usually retains the first d^{*} PCs to ensure the corresponding variances can account for 95% - 99.9% of the total variance. In this way, the dimension of outputs can be reduced from nd to d^{*}. This means one only need to train d^{*} uncorrelated GP models instead of nd highly correlated ones.

In training GP models for the PC scores, each column in $\mathbf{S}^{*}$ serve as a sample. For a new input, the GP model give predictions for the corresponding PC scores $\mathbf{S}^{*}$ can be transformed back from the PC subspace to the original space by the following manipulation:

$$\mathbf{y}^{M} = \mathbf{U}^{*}\mathbf{s}^{*} + \bar{\mathbf{y}}^{M} \tag{48}$$

Appendix B. Algorithm to compute Sobol indices

In this work, the algorithm proposed by (Saltelli, 2002) is used to calculate Sobol indices. Firstly, create two $M \times p$ sample matrices through random sampling, where M is the sample size, p is the number of parameters investigated.

$$\begin{aligned}\mathbf{A} &= \begin{pmatrix} \theta_1^1 & \dots & \theta_i^1 & \dots & \theta_p^1 \\ \vdots & & \vdots & & \vdots \\ \theta_1^M & \dots & \theta_i^M & \dots & \theta_p^M \end{pmatrix}, \\ \mathbf{B} &= \begin{pmatrix} \hat{\theta}_1^1 & \dots & \hat{\theta}_i^1 & \dots & \hat{\theta}_p^1 \\ \vdots & & \vdots & & \vdots \\ \hat{\theta}_1^M & \dots & \hat{\theta}_i^M & \dots & \hat{\theta}_p^M \end{pmatrix}.\end{aligned} \tag{49}$$

Secondly, create p different $M \times p$ matrices based on A and B.

$$C_i = \begin{pmatrix} \hat{\theta}_1^1 & \dots & \theta_i^1 & \dots & \hat{\theta}_p^1 \\ \vdots & & \vdots & & \vdots \\ \hat{\theta}_1^M & \dots & \theta_i^M & \dots & \hat{\theta}_p^M \end{pmatrix}, \tag{50}$$

which is identical to B except the i^{th} column which is taken from A.

Then compute $M \times 1$ vectors of model prediction:

$$y_A = f(A), y_B = f(B), y_C = f(C) \tag{51}$$

The total number of model evaluations is $M(p+2)$.

The first-order sensitivity indices can be estimated as

$$S_i = \frac{\frac{1}{M}\sum_{j=1}^{M} y_A^j y_{C_i}^j - f_0^2}{\frac{1}{M}\sum_{j=1}^{M} (y_A^j)^2 - f_0^2}, \tag{52}$$

where f_0 is the mean of model prediction which can be approximated as

$$f_0^2 = \left(\frac{1}{M}\sum_{j=1}^{M} y_A^j\right)\left(\frac{1}{M}\sum_{j=1}^{M} y_B^j\right). \tag{53}$$

The total sensitivity indices can be estimated as

$$S_{T_i} = 1 - \frac{\frac{1}{M}\sum_{j=1}^{M} y_B^j y_{C_i}^j - f_0^2}{\frac{1}{M}\sum_{j=1}^{M} (y_A^j)^2 - f_0^2}. \tag{54}$$

Appendix C. Parameter selection algorithm

In this work, the parameter selection algorithm proposed by (Banks et al., 2013) is used. The local sensitivity around nominal parameter values $\mathbf{q_0}$ can be analyzed based on the sensitivity matrix which is defined as

$$\chi(\boldsymbol{\theta}_0) = \begin{pmatrix} \frac{\partial y^M}{\partial \theta_1}(x_1, v, \boldsymbol{\theta}_0) & \dots & \frac{\partial y^M}{\partial \theta_p}(x_1, v, \boldsymbol{\theta}_0) \\ \vdots & \ddots & \vdots \\ \frac{\partial y^M}{\partial \theta_1}(x_n, v, \boldsymbol{\theta}_0) & \cdots & \frac{\partial y^M}{\partial \theta_p}(x_n, v, \boldsymbol{\theta}_0) \end{pmatrix} \tag{55}$$

Based on sensitivity matrix $\chi(\boldsymbol{\theta}_0)$, the Fisher information matrix is

$$\mathbf{F}(\boldsymbol{\theta}_0) = \frac{1}{s_0^2}\left(\chi^T(\boldsymbol{\theta}_0)\chi(\boldsymbol{\theta}_0)\right), \tag{56}$$

where s_0^2 is the estimated error variance:

$$s_0^2 = \frac{1}{n-p}\sum_{i=1}^{n}(y^E(v_i) - y^M(v_i, \boldsymbol{\theta}_0))^2 \tag{57}$$

The covariance matrix $\mathbf{V}$ can be estimated as

$$\mathbf{V}(\boldsymbol{\theta}_0) = s_0^2\left(\chi^T(\boldsymbol{\theta}_0)\chi(\boldsymbol{\theta}_0)\right)^{-1} = \mathbf{F}^{-1}(\boldsymbol{\theta}_0). \tag{58}$$

The coefficient of variation can be defined as:

$$v(\boldsymbol{\theta}_0)_i = \frac{\left(\mathbf{V}(\boldsymbol{\theta}_0)_{i,i}\right)^{1/2}}{(\boldsymbol{\theta}_0)_i}, \tag{59}$$

where $\mathbf{V}(\boldsymbol{\theta}_0)_{i,i}$ is the i^{th} diagonal entry in the covariance matrix. The coefficient of variation $v(\boldsymbol{\theta}_0)_i$ represents the ratio of standard error of θ_i to its nominal value. Based on it, the parameter selection score $\beta(\boldsymbol{\theta}_0)$ can be defined as the Euclidean norm of the vector $v(\boldsymbol{\theta}_0)$:

$$\beta(\boldsymbol{\theta}_0) = \|v(\boldsymbol{\theta}_0)\|_{l-2} = \sqrt{\sum_{i=1}^{p} (v(\boldsymbol{\theta}_0)_i)^2} \tag{60}$$

If one wants to select a subset of parameters of size p^* from the whole parameters (of size p), the parameter selection based on $\beta(\boldsymbol{\theta}_0)$ can be accomplished by the following algorithm:

1). For $p^* < p$, consider all possible choices of indices i_1 , i_2,…, i_{p^*} with lexicographical order, which is the enumeration of the combination $\binom{p}{p^*}$.

2). Initialize the minimum selection score $\beta^{sel}=\infty$ and the selected index vector ind^{sel} to be (1,2,…, p^*).

3). Start with the first choice $\left(i_1^{(k)}, i_2^{(k)}, \ldots, i_{p^*}^{(k)}\right)$ and completes the following steps:

Step k: for index $\left(i_1^{(k)}, i_2^{(k)}, \ldots, i_{p^*}^{(k)}\right)$, compute $r = rank(\mathbf{F}(\boldsymbol{\theta}_{0,i_1^{(k)}}, \boldsymbol{\theta}_{0,i_2^{(k)}}, \ldots, \boldsymbol{\theta}_{0,i_{p^*}^{(k)}})$

if $r < p^*$ (which means selected parameters in this step are not mutually identifiable), go to step k+1

if $r = p^*$, compute the corresponding selection score $\beta_k = \beta(\boldsymbol{\theta}_{0,i_1^{(k)}}, \boldsymbol{\theta}_{0,i_2^{(k)}}, \ldots, \boldsymbol{\theta}_{0,i_{p^*}^{(k)}})$:

if $\beta_k > \beta^{sel}$, go to step k+1

if $\beta_k < \beta^{sel}$, set $\beta^{sel}=\beta_k$ and ind^{sel} to be $\left(i_1^{(k)}, i_2^{(k)}, \ldots, i_{p^*}^{(k)}\right)$, then go to step k+1.

Through this algorithm, the subset of parameters with size p^* with minimum selection score can be selected, the low score means low uncertainty probabilities in the estimation. The choice of p^* depends on the rank analysis of the full Fisher information matrix $\mathbf{F}(\boldsymbol{\theta}_0)$.

Nomenclature

A_a	interfacial area concentration, 1/m	*Greek symbols*	
A_b	effective bubble area fraction	α	void fraction
C_d	drag coefficient	Γ_{ki}	Evaporation/condensation rate per volume, kg/(m^3·s)
C_l	lift coefficient	θ	contact angle, rad
C_{wl}	wall lubrication coefficient	σ	surface tension, kg/s^2
C_p	specific heat at constant pressure, J/(kg·K)	σ^t	turbulent dispersion coefficient
C_{vm}	virtual mass coefficient	λ	thermal conductivity, W/(m·K)
D_d	bubble departure diameter, m	μ	dynamic viscosity, Pa·s
D_S	bubble diameter in bulk flow, m	υ	kinematic viscosity, m^2/s
f_d	bubble departure frequency, 1/s	ρ	density, kg/m^3
$\boldsymbol{g}$	Gravity vector, m/s^2	τ	stress tensor, kg/(m·s^2)
h	specific enthalpy, J/kg	Φ	source term of interfacial area concentration, 1/m^3
h_{fg}	latent heat of evaporation, J/kg		
h_l	forced convective heat transfer coefficient, W/(m^2·K)	*Subscripts*	
h_{lg}	interfacial heat transfer coefficient, W/(m^2·K)	g	gas phase
$\boldsymbol{M}$	interfacial force, N/m^3	r	relative motion
N_a	nucleation site density, 1/m^2	sat	saturation
$\boldsymbol{n_w}$	unit vector normal to the wall	sub	subcooling
Pr^t	turbulent Prandtl number	sup	superheat
p	pressure, Pa	l	liquid phase
q_{wall}	wall heat flux, W/m^2		
q_{Ev}	evaporation heat flux, W/m^2	*Superscript*	
q_{Qu}	quenching heat flux, W/m^2	t	turbulence
q_{Fc}	forced convective heat flux, W/m^2		
T	temperature, K		
t	time, s		
$\boldsymbol{U}$	velocity, m/s		
y_w	near wall distance, m		
y^+	dimensionless wall distance		

Acknowledgement

This research was partially supported by the Consortium for Advanced Simulation of Light Water Reactors (http://www.casl.gov), an Energy Innovation Hub (http://www.energy.gov/hubs) for Modeling and Simulation of Nuclear Reactors under U.S. Department of Energy Contract No. DE-AC05-00OR22725. and by Nuclear Energy University Program under the grant DE-NE0008530.

References

AIAA, 1998. Guide for the Verification and Validation of Computational Fluid Dynamics Simulations. American Institute of Aeronautics and Astronautics, AIAA-G-077-1998.

Anglart H., Nylund O., Kurul N., Podowski M.Z., 1997. CFD prediction of flow and phase distribution in fuel assemblies with spacers. Nucl. Eng. Des. 177(1), 215-228.

Antal S.P., Lahey R.T., Flaherty J.E., 1991. Analysis of phase distribution in fully developed laminar bubbly two-phase flow. Int. J. Multiphase Flow. 17(5), 635-652.

Auton T.R., Hunt J., Prud'Homme M., 1988. The force exerted on a body in inviscid unsteady non-uniform rotational flow. J. Fluid Mech. 197, 241-257.

Avramova M.N. and Ivanov K.N., 2010. Verification, validation and uncertainty quantification in multi-physics modeling for nuclear reactor design and safety analysis. Prog. Nuclear Energy. 52(7), 601-614.

Banks H.T., Cintron-Arias A., Kappel F., 2013. Parameter selection methods in inverse problem formulation. Book section in: Mathematical modeling and validation in physiology. Springer.

Basu N., Warrier G.R., Dhir V.K., 2005. Wall heat flux partitioning during subcooled flow boiling: Part 1—model development. Journal of heat Transfer. 127(2), 131-140.

Bayarri M.J., Berger J.O., Paulo R., Sacks J., Cafeo J.A., Cavendish J., Lin C., Tu J., 2007. A framework for validation of computer models. Technometrics. 49(2), 138-154.

Bui A., Williams B., Dinh N., Nourgaliev R., 2013. Statistical modeling support for calibration of a multiphysics model of subcooled boiling flows. in: Proc.International Conference on Mathematics and Computational Methods Applied to Nuclear Science & Engineering, LaGrange Park, IL.

Burns A.D., Frank T., Hamill I., Shi J., 2004. The Favre averaged drag model for turbulent dispersion in Eulerian multi-phase flows. in: Proc.5th international conference on multiphase flow, Yokohama, Japan.

Chen Y.M. and Mayinger F., 1992. Measurement of heat transfer at the phase interface of condensing bubbles. Int. J. Multiphase Flow. 18(6), 877-890.

Cheung S., Vahaji S., Yeoh G.H., Tu J.Y., 2014. Modeling subcooled flow boiling in vertical channels at low pressures - Part 1: Assessment of empirical correlations. Int. J. Heat Mass Transfer. 75, 736-753.

Cole R., 1967. Bubble frequencies and departure volumes at subatmospheric pressures. AIChE J. 13(4), 779-783.

Cole R. and Rohsenow W.M., 1969. Correlation of bubble departure diameters for boiling of saturated liquids. Chem. Eng. Prog. Symp. Ser. 65(92), 211-213.

Colombo M. and Fairweather M., 2016. Accuracy of Eulerian–Eulerian, two-fluid CFD boiling models of subcooled boiling flows. Int. J. Heat Mass Transfer. 103, 28-44.

Constantine P.G., Dow E., Wang Q., 2014. Active subspace methods in theory and practice: applications to kriging surfaces. SIAM J. Sci. Comput. 36(4), A1524.

Del Valle V.H. and Kenning D., 1985. Subcooled flow boiling at high heat flux. Int. J. Heat Mass Transfer. 28(10), 1907-1920.

Donato A. and Pitchumani R., 2014. QUICKER: Quantifying Uncertainty In Computational Knowledge Engineering Rapidly—A rapid methodology for uncertainty analysis. Powder Technol. 265, 54-65.

Feng J. and Bolotnov I.A., 2017. Evaluation of bubble-induced turbulence using direct numerical simulation. Int. J. Multiphase Flow. 93, 92-107.

Ferson S. and Oberkampf W.L., 2009. Validation of imprecise probability models. International Journal of Reliability and Safety. 3(1-3), 3-22.

Ferson S., Oberkampf W.L., Ginzburg L., 2008. Model validation and predictive capability for the thermal challenge problem. Comput. Methods Appl. Mech. Eng. 197(29), 2408-2430.

Gilman L. and Baglietto E., 2017. A self-consistent, physics-based boiling heat transfer modeling framework for use in computational fluid dynamics. Int. J. Multiphase Flow. 95, 35-53.

Gosman A.D., Lekakou C., Politis S., Issa R.I., Looney M.K., 1992. Multidimensional modeling of turbulent two-phase flows in stirred vessels. AIChE J. 38(12), 1946-1956.

Haario H., Laine M., Mira A., Saksman E., 2006. DRAM: efficient adaptive MCMC. Statistics and computing. 16(4), 339-354.

Hibiki T. and Ishii M., 2003. Active nucleation site density in boiling systems. Int. J. Heat Mass Transfer. 46(14), 2587-2601.

Hibiki T. and Ishii M., 2002. Development of one-group interfacial area transport equation in bubbly flow systems. Int. J. Heat Mass Transfer. 45(11), 2351-2372.

Higdon D., Gattiker J., Williams B., Rightley M., 2008. Computer model calibration using high-dimensional output. J. Am. Stat. Assoc. 103(482), 570-583.

Higdon D., Kennedy M., Cavendish J.C., Cafeo J.A., Ryne R.D., 2004. Combining field data and computer simulations for calibration and prediction. SIAM J. Sci. Comput. 26(2), 448-466.

Hoang N.H., Song C., Chu I., Euh D., 2017. A bubble dynamics-based model for wall heat flux partitioning during nucleate flow boiling. Int. J. Heat Mass Transfer. 112, 454-464.

Hosder S., Watson L.T., Grossman B., Mason W.H., Kim H., Haftka R.T., Cox S.E., 2001. Polynomial response surface approximations for the multidisciplinary design optimization of a high speed civil transport. Optim. Eng. 2(4), 431-452.

Ishii M. and Zuber N., 1979. Drag coefficient and relative velocity in bubbly, droplet or particulate flows. AIChE J. 25(5), 843-855.

Kennedy M.C. and O'Hagan A., 2001. Bayesian calibration of computer models. J. Royal Stat. Soc: Series B (Statistical Methodology). 63(3), 425-464.

Kocamustafaogullari G., 1983. Pressure dependence of bubble departure diameter for water. Int. Commun. Heat Mass Transfer. 10(6), 501-509.

Kocamustafaogullari G. and Ishii M., 1995. Foundation of the interfacial area transport equation and its closure relations. Int. J. Heat Mass Transfer. 38(3), 481-493.

Krepper E., Končar B., Egorov Y., 2007. CFD modelling of subcooled boiling—concept, validation and application to fuel assembly design. Nucl. Eng. Des. 237(7), 716-731.

Krepper E., Lucas D., Frank T., Prasser H., Zwart P.J., 2008. The inhomogeneous MUSIG model for the simulation of polydispersed flows. Nucl. Eng. Des. 238(7), 1690-1702.

Kurul N. and Podowski M.Z., 1991. Multidimensional effects in forced convection subcooled boiling. in: Proc.9th International Heat Transfer Conference, Jerusalem, Israel.

Lemmert M. and Chawla J.M., 1977. Influence of flow velocity on surface boiling heat transfer coefficient. Heat Transfer in Boiling. , 237-247.

Liu F., Bayarri M.J., Berger J.O., Paulo R., Sacks J., 2008. A Bayesian analysis of the thermal challenge problem. Comput. Methods Appl. Mech. Eng. 197(29), 2457-2466.

Liu Y., Chen W., Arendt P., Huang H., 2011. Toward a better understanding of model validation metrics. Journal of Mechanical Design. 133(7), 071005.

Ma M., Lu J., Tryggvason G., 2016. Using statistical learning to close two-fluid multiphase flow equations for bubbly flows in vertical channels. Int. J. Multiphase Flow. 85, 336-347.

Mimouni S., Baudry C., Guingo M., Lavieville J., Merigoux N., Mechitoua N., 2016. Computational multi-fluid dynamics predictions of critical heat flux in boiling flow. Nucl. Eng. Des. 299, 28-36.

Morris M.D., 1991. Factorial sampling plans for preliminary computational experiments. Technometrics. 33(2), 161-174.

Nguyen V., Song C., Bae B., Euh D., 2013. Modeling of bubble coalescence and break-up considering turbulent suppression phenomena in bubbly two-phase flow. Int. J. Multiphase Flow. 54, 31-42.

Oberkampf W.L. and Barone M.F., 2006. Measures of agreement between computation and experiment: validation metrics. Journal of Computational Physics. 217(1), 5-36.

Oberkampf W.L. and Roy C.J., 2010. Verification and validation in scientific computing. Cambridge University Press.

Oberkampf W.L. and Smith B.L., 2017. Assessment Criteria for Computational Fluid Dynamics Model Validation Experiments. Journal of Verification, Validation and Uncertainty Quantification. 2(3), 1-14.

Oberkampf W.L. and Trucano T.G., 2002. Verification and validation in computational fluid dynamics. Prog. Aerospace Sci. 38(3), 209-272.

Picchi D. and Poesio P., 2017. Uncertainty quantification and global sensitivity analysis of mechanistic one-dimensional models and flow pattern transition boundaries predictions for two-phase pipe flows. Int. J. Multiphase Flow. 90, 64-78.

Podowski R.M., Drew D.A., Lahey Jr R.T., Podowski M.Z., 1997. A mechanistic model of the ebullition cycle in forced convection subcooled boiling. in: Proc.8th international topical meeting on nuclear reactor thermal-hydraulics, Kyoto, Japan.

Ranz W.E. and Marshall W.R., 1952. Evaporation from drops. Chem. Eng. Prog. 48(3), 141-146.

Ren G., Rafiee J., Aryana S.A., Younis R.M., 2017. A Bayesian model selection analysis of equilibrium and nonequilibrium models for multiphase flow in porous media. Int. J. Multiphase Flow. 89, 313-320.

Roache P.J., 1997. Quantification of uncertainty in computational fluid dynamics. Annu. Rev. Fluid Mech. 29(1), 123-160.

Rzehak R. and Krepper E., 2013. CFD for subcooled flow boiling: Parametric variations. Sci. Technol. Nucl. Install. 2013

Saltelli A., 2002. Making best use of model evaluations to compute sensitivity indices. Comput. Phys. Commun. 145(2), 280-297.

Sato Y. and Sekoguchi K., 1975. Liquid velocity distribution in two-phase bubble flow. Int. J. Multiphase Flow. 2(1), 79-95.

Smith R.C., 2014. Uncertainty quantification: theory, implementation, and applications. SIAM.

Sobol I.M., 2001. Global sensitivity indices for nonlinear mathematical models and their Monte Carlo estimates. Math. Comput. Simul. 55(1), 271-280.

Sugrue R., Magolan B., Lubchenko N., Baglietto E., 2017. Assessment of a simplified set of momentum closure relations for low volume fraction regimes in STAR-CCM and OpenFOAM. Ann. Nucl. Energy. 110, 79-87.

Tolubinsky V.I. and Konstanchuk D.M., 1972. The rate of vapour-bubble growth in boiling of subcooled water. Heat Transfer-Soviet Research. 4(6), 7-12.

Tomiyama A., 1998. Struggle with computational bubble dynamics. Multiph. Sci. Technol. 10(4), 369-405.

Tomiyama A., Kataoka I., Zun I., Sakaguchi T., 1998. Drag coefficients of single bubbles under normal and micro gravity conditions. JSME Int J., Ser. B. 41(2), 472-479.

Wang C.H. and Dhir V.K., 1993. Effect of surface wettability on active nucleation site density during pool boiling of water on a vertical surface. J. Heat Transfer. 115(3), 659-669.

Wang Q. and Yao W., 2016. Computation and validation of the interphase force models for bubbly flow. Int. J. Heat Mass Transfer. 98, 799-813.

Wu X. and Kozlowski T., 2017. Inverse uncertainty quantification of reactor simulations under the Bayesian framework using surrogate models constructed by polynomial chaos expansion. Nucl. Eng. Des. 313, 29-52.

Wu X., Mui T., Hu G., Meidani H., Kozlowski T., 2017. Inverse uncertainty quantification of TRACE physical model parameters using sparse gird stochastic collocation surrogate model. Nucl. Eng. Des. 319, 185-200.

Yadigaroglu G., 2014. CMFD and the critical-heat-flux grand challenge in nuclear thermal–hydraulics–A letter to the Editor of this special issue. Int. J. Multiphase Flow. 67, 3-12.

Yang S.R. and Kim R.H., 1988. A mathematical model of the pool boiling nucleation site density in terms of the surface characteristics. Int. J. Heat Mass Transfer. 31(6), 1127-1135.

Yao W. and Morel C., 2004. Volumetric interfacial area prediction in upward bubbly two-phase flow. Int. J. Heat Mass Transfer. 47(2), 307-328.

Yeoh G.H., Vahaji S., Cheung S., Tu J.Y., 2014. Modeling subcooled flow boiling in vertical channels at low pressures–Part 2: Evaluation of mechanistic approach. Int. J. Heat Mass Transfer. 75, 754-768.

Yurko J.P., Buongiorno J., Youngblood R., 2015. Demonstration of emulator-based Bayesian calibration of safety analysis codes: Theory and formulation. Sci. Technol. Nucl. Install. 2015, 1-17.

Zeng L.Z., Klausner J.F., Bernhard D.M., Mei R., 1993. A unified model for the prediction of bubble detachment diameters in boiling systems—II. Flow boiling. Int. J. Heat Mass Transfer. 36(9), 2271-2279.